Effect of trends on detrended fluctuation analysis

Kun Hu,[1] Plamen Ch. Ivanov,[1,2] Zhi Chen,[1] Pedro Carpena,[3] and H. Eugene Stanley[1]
[1]*Center for Polymer Studies and Department of Physics, Boston University, Boston, Massachusetts 02215*
[2]*Harvard Medical School, Beth Israel Deaconess Medical Center, Boston, Massachusetts 02215*
[3]*Departamento de Física Aplicada II, Universidad de Málaga E-29071, Málaga, Spain*
(Received 8 March 2001; published 26 June 2001)

Detrended fluctuation analysis (DFA) is a scaling analysis method used to estimate long-range power-law correlation exponents in noisy signals. Many noisy signals in real systems display trends, so that the scaling results obtained from the DFA method become difficult to analyze. We systematically study the effects of three types of trends — linear, periodic, and power-law trends, and offer examples where these trends are likely to occur in real data. We compare the difference between the scaling results for artificially generated correlated noise and correlated noise with a trend, and study how trends lead to the appearance of crossovers in the scaling behavior. We find that crossovers result from the competition between the scaling of the noise and the ''apparent'' scaling of the trend. We study how the characteristics of these crossovers depend on (i) the slope of the linear trend; (ii) the amplitude and period of the periodic trend; (iii) the amplitude and power of the power-law trend, and (iv) the length as well as the correlation properties of the noise. Surprisingly, we find that the crossovers in the scaling of noisy signals with trends also follow scaling laws—i.e., long-range power-law dependence of the position of the crossover on the parameters of the trends. We show that the DFA result of noise with a trend can be exactly determined by the superposition of the separate results of the DFA on the noise and on the trend, assuming that the noise and the trend are not correlated. If this superposition rule is not followed, this is an indication that the noise and the superposed trend are not independent, so that removing the trend could lead to changes in the correlation properties of the noise. In addition, we show how to use DFA appropriately to minimize the effects of trends, how to recognize if a crossover indicates indeed a transition from one type to a different type of underlying correlation, or if the crossover is due to a trend without any transition in the dynamical properties of the noise.

DOI: 10.1103/PhysRevE.64.011114 PACS number(s): 05.40.−a

I. INTRODUCTION

Many physical and biological systems exhibit complex behavior characterized by long-range power-law correlations. Traditional approaches such as the power-spectrum and correlation analysis are not suited to accurately quantify long-range correlations in nonstationary signals—e.g., signals exhibiting fluctuations along polynomial trends. Detrended fluctuation analysis (DFA) [1–4] is a scaling analysis method providing a simple quantitative parameter—the scaling exponent α—to represent the correlation properties of a signal. The advantages of DFA over many methods are that it permits the detection of long-range correlations embedded in seemingly nonstationary time series, and also avoids the spurious detection of apparent long-range correlations that are an artifact of nonstationarity. In the past few years, more than 100 publications have utilized the DFA as the method of correlation analysis, and have uncovered long-range power-law correlations in many research fields such as cardiac dynamics [5–23], bioinformatics [1,2,24–34,68], economics [35–47], meteorology [48–50], material science [51], ethology [52], etc. Furthermore, the DFA method may help identify different states of the same system according to its different scaling behaviors, e.g., the scaling exponent α for heart interbeat intervals is different for healthy and sick individuals [14,16,17,53].

The correct interpretation of the scaling results obtained by the DFA method is crucial for understanding the intrinsic dynamics of the systems under study. In fact, for all systems where the DFA method was applied, there are many issues that remain unexplained. One of the common challenges is that the correlation exponent is not always a constant (independent of scale) and crossovers often exist—i.e., a change of the scaling exponent α for different range of scales [5,16,35]. A crossover usually can arise from a change in the correlation properties of the signal at different time or space scales, or can often arise from trends in the data. In this paper we systematically study how different types of trends affect the apparent scaling behavior of long-range correlated signals. The existence of trends in times series generated by physical or biological systems is so common that it is almost unavoidable. For example, the number of particles emitted by a radiation source in a unit time has a trend of decreasing because the source becomes weaker [54,55]; the density of air due to gravity has a trend at a different altitude; the air temperature in different geographic locations, rainfall and the water flow of rivers have a periodic trend due to seasonal changes [49,50,56–59]; the occurrence rate of earthquakes in certain areas has a trend in different time periods [60]. An immediate problem facing researchers applying a scaling analysis to a time series is whether trends in data arise from external conditions, having little to do with the intrinsic dynamics of the system generating noisy fluctuating data. In this case, a possible approach is to first recognize and filter out the trends before we attempt to quantify correlations in the noise. Alternatively, trends may arise from the intrinsic dynamics of the system rather than being an epiphenomenon of external conditions, and thus they may be correlated with

the noisy fluctuations generated by the system. In this case, careful consideration should be given if trends should be filtered out when estimating correlations in the noise, since such ''intrinsic'' trends may be related to the local properties of the noisy fluctuations.

Here we study the origin and the properties of crossovers in the scaling behavior of noisy signals, by applying the DFA method first on correlated noise and then on noise with trends, and comparing the difference in the scaling results. To this end, we generate an artificial time series—anticorrelated, white, and correlated noise with standard deviation equal to one—using the modified Fourier filtering method introduced by Makse *et al.* [63]. We consider the case when the trend is independent of the local properties of the noise (external trend). We find that the scaling behavior of noise with a trend is a superposition of the scaling of the noise and the apparent scaling of the trend, and we derive analytical relations based on the DFA, which we call the ''superposition rule.'' We show how this superposition rule can be used to determine if the trends are independent of the noisy fluctuation in real data, and if filtering these trends out will not affect the scaling properties of the data.

The outline of this paper is as follows. In Sec. II we review the algorithm of the DFA method, and in Appendix A we compare the performance of the DFA with the classical scaling analysis—Hurst's analysis (R/S analysis)—and show that the DFA is a superior method to quantify the scaling behavior of noisy signals. In Sec. III we consider the effect of a linear trend and we present an analytic derivation of the apparent scaling behavior of a linear trend in Appendix C. In Sec. IV we study a periodic trend, and in Sec. V we study the effect of a power-law trend. We systematically study all resulting crossovers, their conditions of existence, and their typical characteristics associated with the different types of trends. In addition, we also show how to use DFA appropriately to minimize or even eliminate the effects of those trends in cases that trends are not choices of the study, that is, trends do not reflect the dynamics of the system but are caused by some ''irrelevant'' background. Finally, Sec. VI contains a summary.

II. DFA

To illustrate the DFA method, we consider a noisy time series, $u(i)$ $(i=1,\ldots,N_{max})$. We integrate the time series $u(i)$,

$$y(j)=\sum_{i=1}^{j}[u(i)-\langle u\rangle], \tag{1}$$

where

$$\langle u\rangle=\frac{1}{N_{max}}\sum_{j=1}^{N_{max}}u(i), \tag{2}$$

and is divided into boxes of equal size n. In each box, we fit the integrated time series by using a polynomial function, $y_{fit}(i)$, which is called the local trend. For order-l DFA (DFA-1 if $l=1$, DFA-2 if $l=2$, etc.), the l-order polynomial function should be applied for the fitting. We detrend the integrated time series $y(i)$ by subtracting the local trend $y_{fit}(i)$ in each box, and we calculate the detrended fluctuation function

$$Y(i)=y(i)-y_{fit}(i). \tag{3}$$

For a given box size n, we calculate the root mean square (rms) fluctuation

$$F(n)=\sqrt{\frac{1}{N_{max}}\sum_{i=1}^{N_{max}}[Y(i)]^2}. \tag{4}$$

The above computation is repeated for box sizes n (different scales) to provide a relationship between $F(n)$ and n. A power-law relation between $F(n)$ and the box size n indicates the presence of scaling: $F(n)\sim n^{\alpha}$. The parameter α, called the scaling exponent or correlation exponent, represents the correlation properties of the signal: if $\alpha=0.5$, there is no correlation and the signal is an uncorrelated signal (white noise); if $\alpha<0.5$, the signal is anticorrelated; if $\alpha>0.5$, there are positive correlations in the signal.

III. NOISE WITH LINEAR TRENDS

First we consider the simplest case: correlated noise with a linear trend. A linear trend

$$u(i)=A_{\mathrm{L}}i \tag{5}$$

is characterized by only one variable — the slope of the trend A_{L}. For convenience, we denote the rms fluctuation function for noise without trends by $F_{\eta}(n)$, linear trends by $F_{\mathrm{L}}(n)$, and noise with a linear trend by $F_{\eta L}(n)$.

A. DFA-1 on noise with a linear trend

Using the algorithm of Makse *et al.* [63], we generate a correlated noise with a standard deviation one, with a given correlation property characterized by a given scaling exponent α. We apply DFA-1 to quantify the correlation properties of the noise and find that only in a certain good fit region can the rms fluctuation function $F_{\eta}(n)$ be approximated by a power-law function (see Appendix A)

$$F_{\eta}(n)=b_0 n^{\alpha}, \tag{6}$$

where b_0 is a parameter independent of the scale n. We find that the good fit region depends on the correlation exponent α (see Appendix A). We also derive analytically the rms fluctuation function for a linear trend only for DFA-1 and find that (see Appendix C)

$$F_{\mathrm{L}}(n)=k_0 A_{\mathrm{L}} n^{\alpha_L}, \tag{7}$$

where k_0 is a constant independent of the length of trend N_{max}, of the box size n, and of the slope of the trend A_{L}. We obtain $\alpha_L=2$.

Next we apply the DFA-1 method to the superposition of a linear trend with correlated noise and we compare the rms fluctuation function $F_{\eta L}(n)$ with $F_{\eta}(n)$ (see Fig. 1). We

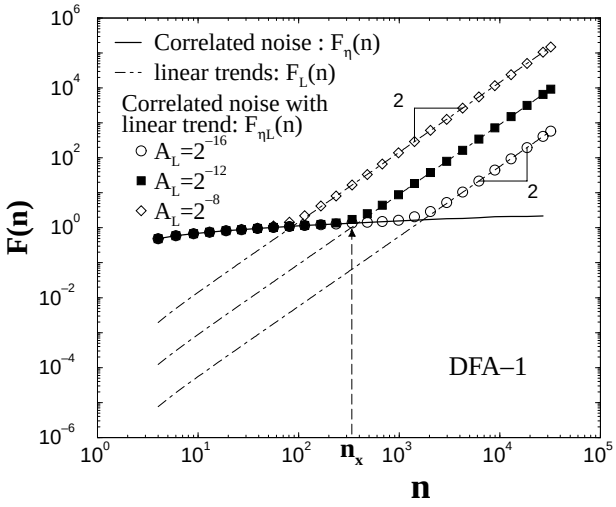

FIG. 1. Crossover behavior of the root-mean-square fluctuation function $F_{\eta L}(n)$ for noise (of length $N_{max}=2^{17}$ and correlation exponent $\alpha=0.1$) with superposed linear trends of slope $A_{\mathrm{L}}=2^{-16},2^{-12},2^{-8}$. For comparison, we show $F_{\eta}(n)$ for the noise (thick solid line) and $F_{\mathrm{L}}(n)$ for the linear trends (dot-dashed line) [Eq. (7)]. The results show a crossover at a scale $n_{\times}$ for $F_{\eta L}(n)$. For $n<n_{\times}$, the noise dominates and $F_{\eta L}(n)\approx F_{\eta}(n)$. For $n>n_{\times}$, the linear trend dominates and $F_{\eta L}(n)\approx F_{\mathrm{L}}(n)$. Note that the crossover scale $n_{\times}$ increases when the slope A_{L} of the trend decreases.

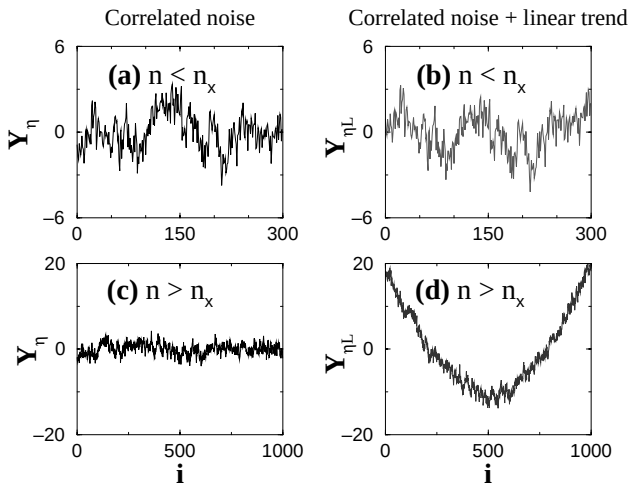

FIG. 2. Comparison of the detrended fluctuation function for noise $Y_{\eta}(i)$ and for noise with linear trend $Y_{\eta L}(i)$ at different scales. (a) and (c) are Y_{η} for noise with $\alpha=0.1$; (b) and (d) are $Y_{\eta L}$ for the same noise with a linear trend with slope $A_{\mathrm{L}}=2^{-12}$ (the crossover scale $n_{\times}=320$, see Fig. 1). (a) and (b) For scales $n<n_{\times}$ the effect of the trend is not pronounced and $Y_{\eta}\approx Y_{\eta L}$ (i.e., $Y_{\eta}\gg Y_{\mathrm{L}}$). (c) and (d) For scales $n>n_{\times}$, the linear trend is dominant and $Y_{\eta}\ll Y_{\eta L}$.

observe a crossover in $F_{\eta L}(n)$ at scale $n=n_{\times}$. For $n<n_{\times}$, the behavior of $F_{\eta L}(n)$ is very close to the behavior of $F_{\eta}(n)$, while for $n>n_{\times}$, the behavior of $F_{\eta L}(n)$ is very close to the behavior of $F_{\mathrm{L}}(n)$. A similar crossover behavior is also observed in the scaling of the well-studied biased random walk [61,62]. It is known that the crossover in the biased random walk is due to the competition of the unbiased random walk and the bias (see Fig. 5.3 of [62]). We illustrate this observation in Fig. 2, where the detrended fluctuation functions [Eq. (3)] of the correlated noise, $Y_{\eta}(i)$, and of the noise with a linear trend, $Y_{\eta L}(i)$, are shown. For the box size $n<n_{\times}$ as shown in Figs. 2(a) and 2(b), $Y_{\eta L}(i)\approx Y_{\eta}(i)$. For $n>n_{\times}$ as shown in Figs. 2(c) and 2(d), $Y_{\eta L}(i)$ has a distinguishable quadratic background significantly different from $Y_{\eta}(i)$. This quadratic background is due to the integration of the linear trend within the DFA procedure and represents the detrended fluctuation function Y_L of the linear trend. These relations between the detrended fluctuation functions $Y(i)$ at different time scales n explain the crossover in the scaling behavior of $F_{\eta L}(n)$: from very close to $F_{\eta}(n)$ to very close to $F_{\mathrm{L}}(n)$ (observed in Fig. 1).

The experimental results presented in Figs. 1 and 2 suggest that the rms fluctuation function for a signal which is a superposition of a correlated noise and a linear trend can be expressed as

$$[F_{\eta L}(n)]^2=[F_{\mathrm{L}}(n)]^2+[F_{\eta}(n)]^2. \tag{8}$$

We provide an analytic derivation of this relation in Appendix B, where we show that Eq. (8) holds for the superposition of any two independent signals—in this particular case noise and a linear trend. We call this relation the ''superposition rule.'' This rule helps us understand how the competition between the contribution of the noise and the trend to the rms fluctuation function $F_{\eta L}(n)$ at different scales n leads to appearance of crossovers [61].

Next, we ask how the crossover scale $n_{\times}$ depends on (i) the slope of the linear trend A_{L}, (ii) the scaling exponent α of the noise, and (iii) the length of the signal N_{max}. Surprisingly, we find that for noise with any given correlation exponent α the crossover scale $n_{\times}$ itself follows a power-law scaling relation over several decades: $n_{\times}\sim(A_{\mathrm{L}})^{\theta}$ (see Fig. 3). We find that in this scaling relation, the crossover exponent θ is negative and its value depends on the correlation exponent α of the noise—the magnitude of θ decreases when α increases. We present the values of the ''crossover exponent'' θ for different correlation exponents α in Table I.

To understand how the crossover scale depends on the correlation exponent α of the noise we employ the superposition rule [Eq. (8)] and estimate $n_{\times}$ as the intercept between $F_{\eta}(n)$ and $F_{\mathrm{L}}(n)$. From Eqs. (6) and (7), we obtain the following dependence of $n_{\times}$ on α:

$$n_{\times}=\left(A_{\mathrm{L}}\frac{k_0}{b_0}\right)^{1/(\alpha-\alpha_L)}=\left(A_{\mathrm{L}}\frac{k_0}{b_0}\right)^{1/(\alpha-2)}. \tag{9}$$

This analytical calculation for the crossover exponent $-1/(\alpha_L-\alpha)$ is in a good agreement with the observed values of θ obtained from our simulations (see Fig. 3 and Table I).

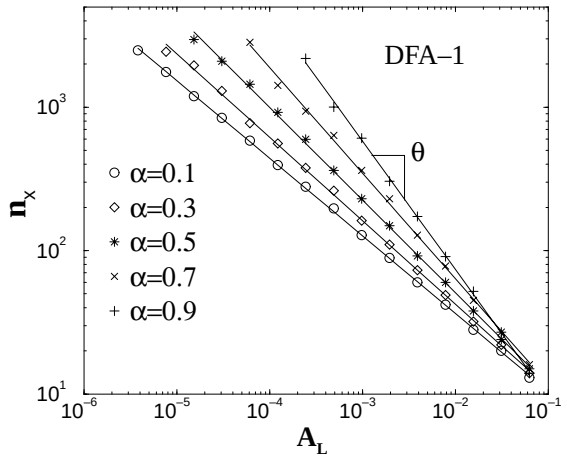

FIG. 3. The crossover $n_\times$ of $F_{\eta L}(n)$ for noise with a linear trend. We determine the crossover scale $n_\times$ based on the difference Δ between $\log F_\eta$ (noise) and $\log F_{\eta L}$ (noise with a linear trend). The scale for which $\Delta = 0.05$ is the estimated crossover scale $n_\times$. For any given correlation exponent α of the noise, the crossover scale $n_\times$ exhibits a long-range power-law behavior $n_\times \sim (A_L)^\theta$, where the crossover exponent θ is a function of α [see Eq. (9) and Table I].

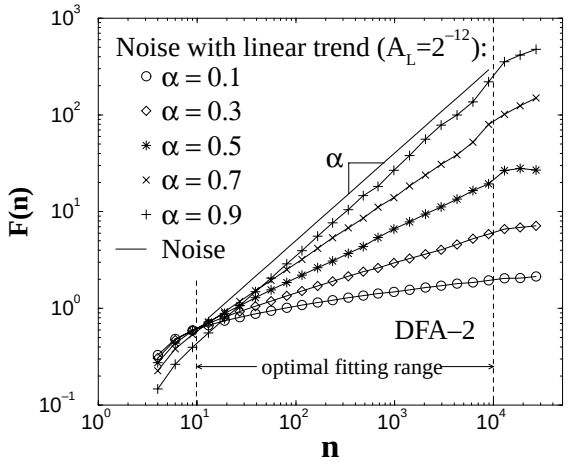

FIG. 4. Comparison of the rms fluctuation function $F_\eta(n)$ for noise with different types of correlations (lines) and $F_{\eta L}(n)$ for the same noise with a linear trend of slope $A_L = 2^{-12}$ (symbols) for DFA-2. $F_{\eta L}(n) = F_\eta(n)$ because the integrated linear trend can be perfectly filtered out in DFA-2, thus $Y_L(i) = 0$ from Eq. (3). We note that to estimate accurately the correlation exponents, one has to choose an optimal range of scales n, where $F(n)$ is fitted. For details see Appendix A.

Finally, since the $F_L(n)$ does not depend on N_{max} as we show in Eq. (7) and in Appendix C, we find that $n_\times$ does not depend on N_{max}. This is a special case for linear trends and does not always hold for higher-order polynomial trends (see Appendix D).

B. DFA-2 on noise with a linear trend

Application of the DFA-2 method to noisy signals without any polynomial trends leads to scaling results identical to the scaling obtained from the DFA-1 method, with the exception of some vertical shift to lower values for the rms fluctuation function $F_\eta(n)$ (see Appendix A). However, for signals which are a superposition of correlated noise and a linear trend, in contrast to the DFA-1 results presented in Fig. 1, $F_{\eta L}(n)$ obtained from DFA exhibits no crossovers, and is exactly equal to the rms fluctuation function $F_\eta(n)$ obtained from DFA-2 for correlated noise without trend (see Fig. 4). These results indicate that a linear trend has no effect on the scaling obtained from DFA-2. The reason for this is that by design the DFA-2 method filters out linear trends, i.e., $Y_L(i) = 0$ [Eq. (3)] and thus $F_{\eta L}(n) = F_\eta(n)$ due to the superposition rule [Eq. (8)]. For the same reason, polynomial trends of order lower than l superposed on correlated noise will have no effect on the scaling properties of the noise when DFA-l is applied. Therefore, our results confirm that the DFA method is a reliable tool to accurately quantify correlations in noisy signals embedded in polynomial trends. Moreover, the reported scaling and crossover features of $F(n)$ can be used to determine the order of polynomial trends present in the data.

TABLE I. The crossover exponent θ from the power-law relation between the crossover scale $n_\times$ and the slope of the linear trend A_L, $n_\times \sim (A_L)^\theta$, for different values of the correlation exponents α of the noise (Fig. 3). The values of θ obtained from our simulations are in good agreement with the analytical prediction $-1/(2-\alpha)$ [Eq. (9)]. Note that $-1/(2-\alpha)$ are not always exactly equal to θ because $F_\eta(n)$ in simulations is not a perfect simple power-law function and the way we determine numerically $n_\times$ is just approximated.

α	θ	$-1/(2-\alpha)$
0.1	-0.54	-0.53
0.3	-0.58	-0.59
0.5	-0.65	-0.67
0.7	-0.74	-0.77
0.9	-0.89	-0.91

IV. NOISE WITH SINUSOIDAL TREND

In this section we study the effect of sinusoidal trends on the scaling properties of noisy signals. For a signal which is a superposition of correlated noise and sinusoidal trend, we find that based on the superposition rule (Appendix B) the DFA rms fluctuation function can be expressed as

$$[F_{\eta S}(n)]^2 = [F_\eta(n)]^2 + [F_S(n)]^2, \tag{10}$$

where $F_{\eta S}(n)$ is the rms fluctuation function of noise with a sinusoidal trend, and $F_S(n)$ is for the sinusoidal trend. First we consider the application of DFA-1 to a sinusoidal trend. Next we study the scaling behavior and the features of crossovers in $F_{\eta S}(n)$ for the superposition of a correlated noise and a sinusoidal trend employing the superposition rule [Eq. (10)]. At the end of this section we discuss the results obtained from higher-order DFA.

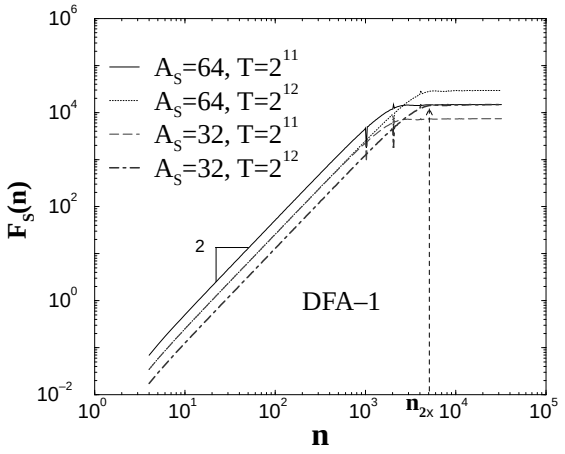

FIG. 5. Root-mean-square fluctuation function $F_S(n)$ for sinusoidal functions of length $N_{max}=2^{17}$ with different amplitude A_S and period T. All curves exhibit a crossover at $n_{2\times}\approx T/2$, with a slope $\alpha_S=2$ for $n<n_{2\times}$ and a flat region for $n>n_{2\times}$. There are some spurious singularities at $n=j(T/2)$ (j is a positive integer) shown by the spikes.

A. DFA-1 on sinusoidal trend

Given a sinusoidal trend $u(i)=A_S\sin(2\pi i/T)$ ($i=1,\ldots,N_{max}$), where A_S is the amplitude of the signal and T is the period, we find that the rms fluctuation function $F_S(n)$ does not depend on the length of the signal N_{max}, and has the same shape for different amplitudes and different periods [Fig. 5]. We find a crossover at scale corresponding to the period of the sinusoidal trend

$$n_{2\times}\approx T, \tag{11}$$

and it does not depend on the amplitude A_S. We call this crossover $n_{2\times}$ for convenience, as we will see later. For $n<n_{2\times}$, the rms fluctuation $F_S(n)$ exhibits an apparent scaling with the same exponent as $F_L(n)$ for the linear trend [see Eq. (7)],

$$F_S(n)=k_1\frac{A_S}{T}n^{\alpha_S}, \tag{12}$$

where k_1 is a constant independent of the length N_{max}, of the period T, of the amplitude A_S of the sinusoidal signal, and of the box size n. As for the linear trend [Eq. (7)], we obtain $\alpha_S=2$ because at small scales (box size n) the sinusoidal function is dominated by a linear term. For $n>n_{2\times}$, due to the periodic property of the sinusoidal trend, $F_S(n)$ is a constant independent of the scale n,

$$F_S(n)=\frac{1}{2\sqrt{2}\pi}A_S T. \tag{13}$$

The period T and the amplitude A_S also affects the vertical shift of $F_S(n)$ in both regions. We note that in Eqs. (12) and (13), $F_S(n)$ is proportional to the amplitude A_S, a behavior which is also observed for the linear trend [Eq. (7)].

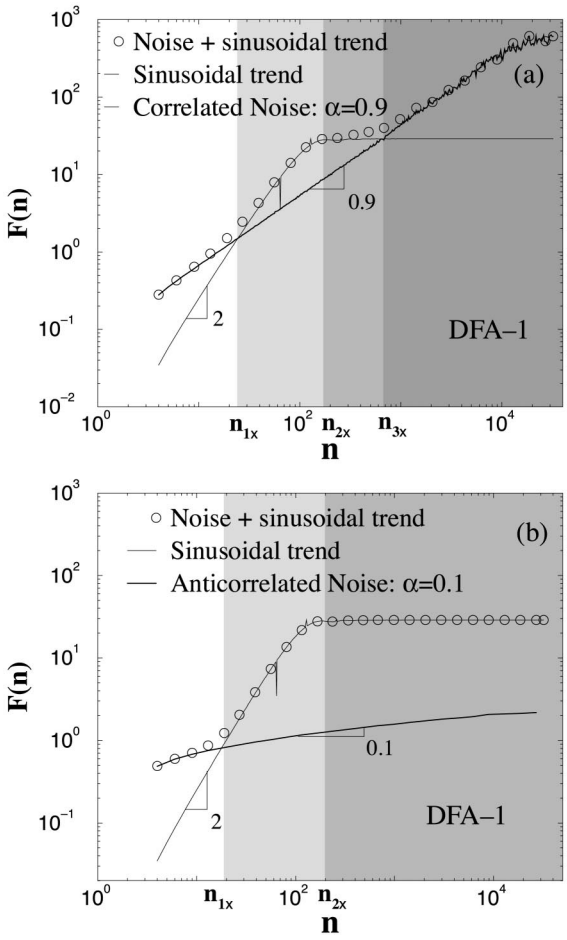

FIG. 6. Crossover behavior of the root-mean-square fluctuation function $F_{\eta S}(n)$ (circles) for correlated noise (of length $N_{max}=2^{17}$) with a superposed sinusoidal function characterized by period $T=128$ and amplitude $A_S=2$. The rms fluctuation function $F_\eta(n)$ for noise (thick line) and $F_S(n)$ for the sinusoidal trend (thin line) are shown for comparison. (a) $F_{\eta S}(n)$ for correlated noise with $\alpha=0.9$. (b) $F_{\eta S}(n)$ for anticorrelated noise with $\alpha=0.9$. There are three crossovers in $F_{\eta S}(n)$, at scales $n_{1\times}$, $n_{2\times}$, and $n_{3\times}$ [the third crossover cannot be seen in (b) because it occurs at scale larger than the length of the signal]. For $n<n_{1\times}$ and $n>n_{3\times}$ the noise dominates and $F_{\eta S}(n)\approx F_\eta(n)$ while for $n_{1\times}<n<n_{3\times}$ the sinusoidal trend dominates and $F_{\eta S}(n)\approx F_S(n)$. The crossovers at $n_{1\times}$ and $n_{3\times}$ are due to the competition between the correlated noise and the sinusoidal trend (see Fig. 7), while the crossover at $n_{2\times}$ relates only to the period T of the sinusoidal [Eq. (11)].

B. DFA-1 on noise with sinusoidal trend

In this section we study how the sinusoidal trend affects the scaling behavior of noise with different types of correlations. We apply the DFA-1 method to a signal which is a superposition of correlated noise with a sinusoidal trend. We observe that there are typically three crossovers in the rms fluctuation $F_{\eta S}(n)$ at characteristic scales denoted by $n_{1\times}$, $n_{2\times}$, and $n_{3\times}$ (Fig. 6). These three crossovers divide $F_{\eta S}(n)$ into four regions, as shown in Fig. 6(a) [the third crossover cannot be seen in Fig. 6(b) because its scale $n_{3\times}$ is greater than the length of the signal]. We find that the first and third

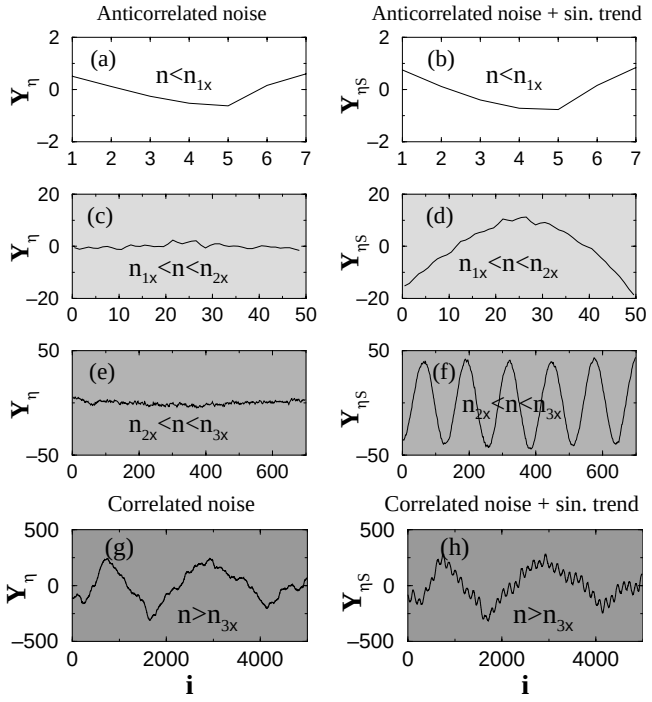

FIG. 7. Comparison of the detrended fluctuation function for noise $Y_\eta(i)$ and noise with sinusoidal trend $Y_{\eta S}(i)$ in four regions as shown in Fig. 6. The same signals as in Fig. 6 are used. Panels (a)–(f) correspond to Fig. 6(b) for anticorrelated noise with exponent $\alpha=0.1$, and panels (g) and (h) correspond to Fig. 6(a) for correlated noise with exponent $\alpha=0.9$. (a) and (b) For all scales $n<n_{1\times}$, the effect of the trend is not pronounced and $Y_{\eta S}(i) \approx Y_\eta(i)$ leading to $F_{\eta S}(n)\approx F_\eta(n)$ [Fig. 6(a)]. (c) and (d) For $n_{2\times}>n>n_{1\times}$ the trend is dominant, $Y_{\eta S}(i)\gg Y_\eta(i)$ and $F_{\eta S}(n) \approx F_S(n)$. Since $n_{2\times}\approx T/2$ [Eq. (11)], the scale $n<T/2$ and the sinusoidal behavior can be approximated as a linear trend. This explains the quadratic background in $Y_{\eta S}(i)$ (d) [see Figs. 2(c) and 2(d)]. (e) and (f) For $n_{2\times}<n<n_{3\times}$ (i.e., $n\gg T/2$), the sinusoidal trend again dominates—$Y_{\eta S}(i)$ is periodic function with period T. (g) and (h) For $n>n_{3\times}$, the effect of the noise is dominant and the scaling of $F_{\eta S}$ follows the scaling of F_η [Fig. 6(a)].

crossovers at scales $n_{1\times}$ and $n_{3\times}$, respectively (see Fig. 6), result from the competition between the effects on $F_{\eta S}(n)$ of the sinusoidal signal and the correlated noise. For $n<n_{1\times}$ (region I) and $n>n_{3\times}$ (region IV), we find that the noise has the dominating effect $[F_\eta(n)>F_S(n)]$, so the behavior of $F_{\eta S}(n)$ is very close to the behavior of $F_\eta(n)$ [Eq. (10)]. For $n_{1\times}<n<n_{2\times}$ (region II) and $n_{2\times}<n<n_{3\times}$ (region III) the sinusoidal trend dominates $[F_S(n)>F_\eta(n)]$, thus the behavior of $F_{\eta S}(n)$ is close to $F_S(n)$ (see Figs. 6 and 7).

To better understand why there are different regions in the behavior of $F_{\eta S}(n)$, we consider the detrended fluctuation function [Eq. (3) and Appendix B] of the correlated noise $Y_\eta(i)$, and of the noise with sinusoidal trend $Y_{\eta S}$. In Fig. 7 we compare $Y_\eta(i)$ and $Y_{\eta S}(i)$ for anticorrelated and correlated noise in the four different regions. For very small scales $n<n_{1\times}$, the effect of the sinusoidal trend is not pronounced, $Y_{\eta S}(i)\approx Y_\eta(i)$, indicating that in this scale region the signal can be considered as noise fluctuating around a constant trend which is filtered out by the DFA-1 procedure [Figs. 7(a) and 7(b)]. Note that the behavior of $Y_{\eta S}$ [Fig. 7(b)] is identical to the behavior of $Y_{\eta L}$ [Fig. 2(b)], since both a sinusoidal with a large period T and a linear trend with small slope A_L can be well approximated by a constant trend for $n<n_{1\times}$. For small scales $n_{1\times}<n<n_{2\times}$ (region II), we find that there is a dominant quadratic background for $Y_{\eta S}(i)$ [Fig. 7(d)]. This quadratic background is due to the integration procedure in DFA-1, and is represented by the detrended fluctuation function of the sinusoidal trend $Y_S(i)$. It is similar to the quadratic background observed for linear trend $Y_{\eta L}(i)$ [Fig. 2(d)]—i.e., for $n_{1\times}<n<n_{2\times}$ the sinusoidal trend behaves as a linear trend and $Y_S(i)\approx Y_L(i)$. Thus in region II the ''linear trend'' effect of the sinusoidal is dominant, $Y_S > Y_\eta$, which leads to $F_{\eta S}(n)\approx F_S(n)$. This explains also why $F_{\eta S}(n)$ for $n<n_{2\times}$ (Fig. 6) exhibits crossover behavior similar to the one of $F_{\eta L}(n)$ observed for noise with a linear trend. For $n_{2\times}<n<n_{3\times}$ (region III) the sinusoidal behavior is strongly pronounced [Fig. 7(f)], $Y_S(i)\gg Y_\eta(i)$, and $Y_{\eta S}(i)\approx Y_S(i)$ changes periodically with period equal to the period of the sinusoidal trend T. Since $Y_{\eta S}(i)$ is bounded between a minimum and a maximum value, $F_{\eta S}(n)$ cannot increase and exhibits a flat region (Fig. 6). At very large scales, $n>n_{3\times}$, the noise effect is again dominant [$Y_S(i)$ remains bounded, while Y_η grows when increasing the scale] which leads to $F_{\eta S}(n)\approx F_\eta(n)$ and a scaling behavior that corresponds to the scaling of the correlated noise.

First we consider $n_{1\times}$. Surprisingly, we find that for noise with any given correlation exponent α the crossover scale $n_{1\times}$ exhibits long-range power-law dependence of the period T, $n_{1\times}\sim T^{\theta_{T1}}$, and the amplitude A_S, $n_{1\times}\sim(A_S)^{\theta_{A1}}$ of the sinusoidal trend [see Figs. 8(a) and 8(b)]. We find that the ''crossover exponents'' θ_{T1} and θ_{A1} have the same magnitude but different sign—θ_{T1} is positive while θ_{A1} is negative. We also find that the magnitudes of θ_{T1} and θ_{A1} increase for larger values of the correlation exponents α of the noise. We present the values of θ_{T1} and θ_{A1} for the different correlation exponents α in Table II. To understand the power-law relations between $n_{1\times}$ and T, between $n_{1\times}$ and A_S, and also how the crossover scale $n_{1\times}$ depends on the correlation exponent α, we employ the superposition rule [Eq. (10)] and estimate $n_{1\times}$ analytically as the first intercept of $F_\eta(n)$ and $F_S(n)$. From Eqs. (12) and (6), we obtain the following dependence of $n_{1\times}$ on T, A_S and α:

$$n_{1\times}=\left(\frac{b_0}{k_1}\frac{T}{A_S}\right)^{1/(2-\alpha)} \tag{14}$$

From this analytical calculation we obtain the following relation between the two crossover exponents θ_{T1} and θ_{A1} and the correlation exponent α: $\theta_{T1}=-\theta_{A1}=1/(2-\alpha)$, which is in a good agreement with the observed values of θ_{T1}, θ_{A1} obtained from simulations [see Figs. 8(a) and 8(b) and Table II].

Next we consider $n_{2\times}$. Our analysis of the rms fluctuation function $F_S(n)$ for the sinusoidal signal in Fig. 5 suggests that the crossover scale $F_S(n)$ does not depend on the-

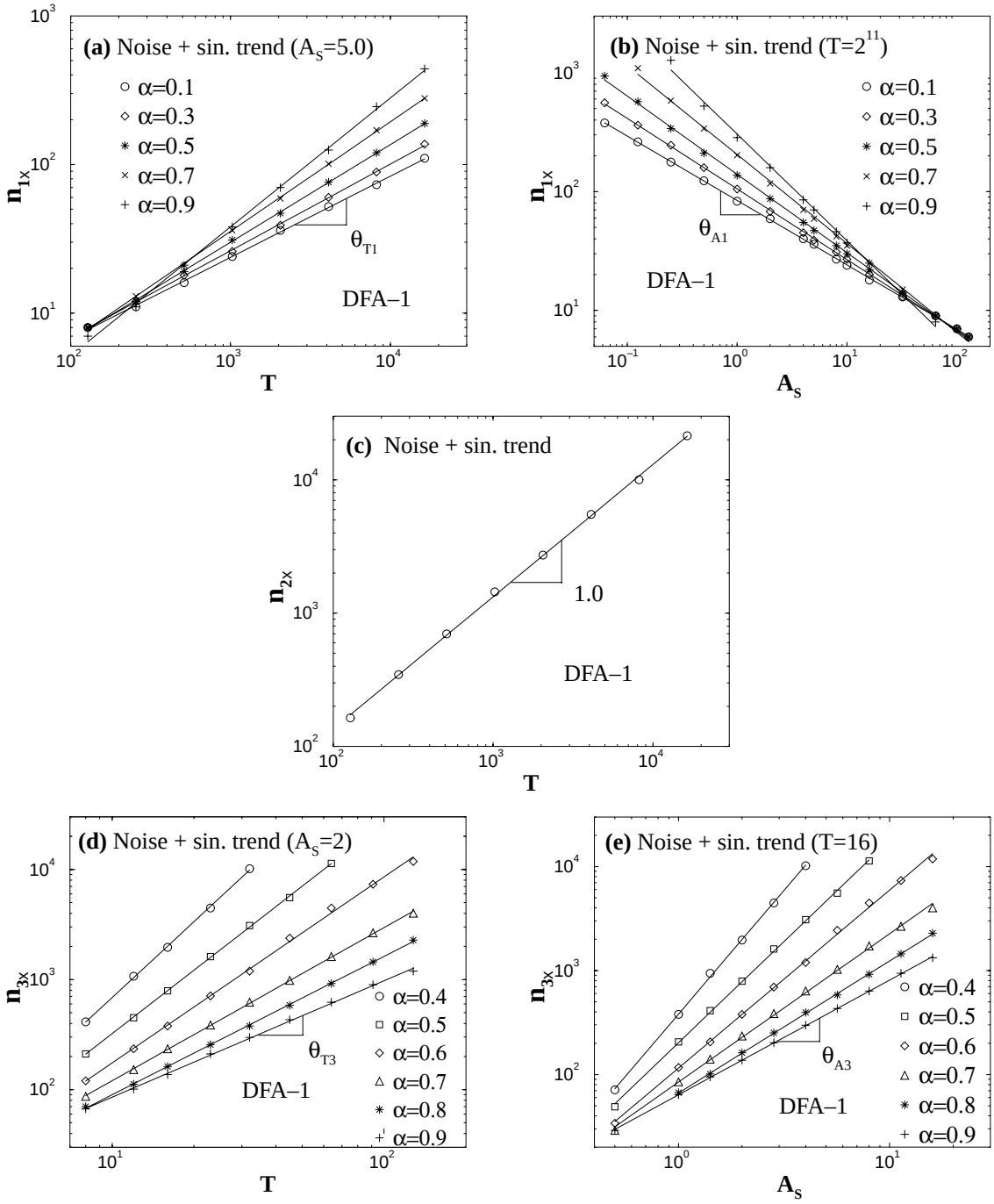

FIG. 8. Dependence of the three crossovers in $F_{\eta S}(n)$ for noise with a sinusoidal trend (Fig. 6) on the period T and amplitude A_S of the sinusoidal trend. (a) Power-law relation between the first crossover scale $n_{1\times}$ and the period T for fixed amplitude A_S and varying correlation exponent α: $n_{1\times}\sim T^{\theta_{T1}}$, where θ_{T1} is a positive crossover exponent [see Table II and Eq. (14)]. (b) Power-law relation between the first crossover $n_{1\times}$ and the amplitude of the sinusoidal trend A_S for fixed period T and varying correlation exponent α: $n_{1\times}\sim A_S^{\theta_{A1}}$ where θ_{A1} is a negative crossover exponent [Table II and Eq. (14)]. (c) The second crossover scale $n_{2\times}$ depends only on the period T: $n_{2\times}\sim T^{\theta_{T2}}$, where $\theta_{T2}\approx 1$. (d) Power-law relation between the third crossover $n_{3\times}$ and T for fixed amplitude A_S and varying α trend: $n_{3\times}\sim T^{\theta_{T3}}$. (e) Power-law relation between the third crossover $n_{3\times}$ and A_S for fixed T and varying α: $n_{3\times}\sim(A_S)^{\theta_{A3}}$. We find that $\theta_{A3}=\theta_{T3}$ [Table III and Eq. (15)].

amplitude A_S of the sinusoidal. The behavior of the rms fluctuation function $F_{\eta S}(n)$ for noise with a superposed sinusoidal trend in Figs. 6(a) and 6(b) indicates that $n_{2\times}$ does not depend on the correlation exponent α of the noise, since for both correlated ($\alpha=0.9$) and anticorrelated ($\alpha=0$) noise (T and A_S are fixed), the crossover scale $n_{2\times}$ remains unchanged. We find that $n_{2\times}$ depends *only* on the period T of the sinusoidal trend and exhibits a long-range power-law behavior $n_{2\times}\sim T^{\theta_{T2}}$ with a crossover exponent $\theta_{T2}\approx 1$ [Fig. 8(c)] which is in agreement with the prediction of Eq. (11).

TABLE II. The crossover exponents θ_{T1} and θ_{A1} characterizing the power-law dependence of $n_{1\times}$ on the period T and amplitude A_S obtained from simulations: $n_{1\times}\sim T^{\theta_{T1}}$ and $n_{1\times}\sim(A_S)^{\theta_{A1}}$ for different values of the correlation exponent α of noise [Figs. 8(a) and 8(b)]. The values of θ_{T1} and θ_{A1} are in good agreement with the analytical predictions $\theta_{T1}=-\theta_{A1}=1/(2-\alpha)$ [Eq. (14)].

α	θ_{T1}	$-\theta_{A1}$	$1/(2-\alpha)$
0.1	0.55	0.54	0.53
0.3	0.58	0.59	0.59
0.5	0.66	0.66	0.67
0.7	0.74	0.75	0.77
0.9	0.87	0.90	0.91

For the third crossover scale $n_{3\times}$, as for $n_{1\times}$ we find a power-law dependence on the period T, $n_{3\times}\sim T^{\theta_{T3}}$, and on the amplitude A_S, $n_{3\times}\sim(A_S)^{\theta_{A3}}$, of the sinusoidal trend [see Figs. 8(d) and 8(e)]. However, in contrast to the $n_{1\times}$ case, we find that the crossover exponents θ_{Tp3} and θ_{A3} are equal and positive with decreasing values for increasing correlation exponents α. In Table III we present the values of these two exponents for different correlation exponent α. To understand how the scale $n_{3\times}$ depends on T, A_S, and the correlation exponent α simultaneously, we again employ the superposition rule [Eq. (10)] and estimate $n_{3\times}$ as the second intercept $n_{3\times}^{th}$ of $F_\eta(n)$ and $F_S(n)$. From Eqs. (13) and (6), we obtain the following dependence:

$$n_{3\times}=\left(\frac{1}{2\sqrt{2}\pi b_0}A_S T\right)^{1/\alpha}. \tag{15}$$

From this analytical calculation we obtain $\theta_{T3}=\theta_{A3}=1/\alpha$ which is in good agreement with the values of θ_{T3} and θ_{A3} observed from simulations (Table III). Finally, our simulations show that all three crossover scales $n_{1\times}$, $n_{2\times}$, and $n_{3\times}$ do not depend on the length of the signal N_{max}, since $F_\eta(n)$ and $F_S(n)$ do not depend on N_{max} as shown in Eqs. (6), (10), (12), and (13).

C. Higher-order DFA on pure sinusoidal trend

In Sec. IV B we discussed how sinusoidal trends affect the scaling behavior of correlated noise when the DFA-1 method is applied. Since DFA-1 removes only constant trends in data, it is natural to ask how the observed scaling results will change when we apply DFA of order l designed to remove polynomial trends of order lower than l. In this section we first consider the rms fluctuation F_S for a sinusoidal signal and then we study the scaling and crossover properties of $F_{\eta S}$ for correlated noise with a superposed sinusoidal signal when higher-order DFA is used.

TABLE III. The crossover exponents θ_{T3} and θ_{A3} for the power-law relations: $n_{3\times}\sim T^{\theta_{T3}}$ and $n_{3\times}\sim(A_S)^{\theta_{A3}}$ for different values of the correlation exponent α of noise [Figs. 8(c) and 8(d)]. The values of θ_{p3} and θ_{a3} obtained from simulations are in good agreement with the analytical predictions $\theta_{T3}=\theta_{A3}=1/\alpha$ [Eq. (15)].

α	θ_{T3}	θ_{A3}	$1/\alpha$
0.4	2.29	2.38	2.50
0.5	1.92	1.95	2.00
0.6	1.69	1.71	1.67
0.7	1.39	1.43	1.43
0.8	1.26	1.27	1.25
0.9	1.06	1.10	1.11

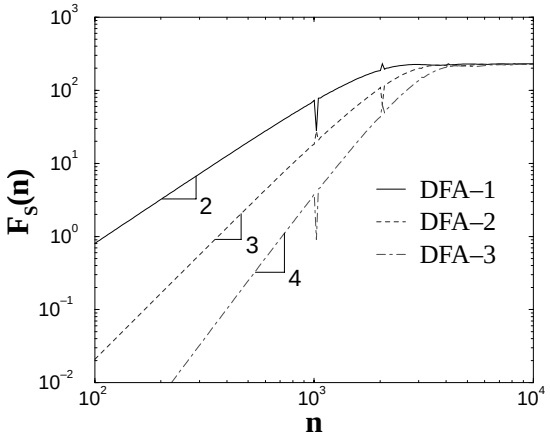

FIG. 9. Comparison of the results of different order DFA on a sinusoidal trend. The sinusoidal trend is given by the function $64\sin(2\pi i/2^{11})$ and the length of the signal is $N_{max}=2^{17}$. The spurious singularities (spikes) arise from the discrete data we use for the sinusoidal function.

We find that the rms fluctuation function F_S does not depend on the length of the signal N_{max}, and preserves a similar shape when a different order-l DFA method is used (Fig. 9). In particular, F_S exhibits a crossover at a scale $n_{2\times}$ proportional to the period T of the sinusoidal: $n_{2\times}\sim T^{\theta_{T2}}$ with $\theta_{T2}\approx 1$. The crossover scale shifts to larger values for higher order l (Figs. 5 and 9). For the scale $n<n_{2\times}$ F_S exhibits an apparent scaling: $F_S\sim n^{\alpha_S}$ with an effective exponent $\alpha_S=l+1$. For DFA-1, we have $l=1$ and recover $\alpha_S=2$ as shown in Eq. (12). For $n>n_{2\times}$, $F_S(n)$ is a constant independent of the scale n and of the order l of the DFA method in agreement with Eq. (13).

Next, we consider $F_{\eta S}(n)$ when DFA-l with a higher order l is used. We find that for all orders l, $F_{\eta S}(n)$ does not depend on the length of the signal N_{max} and exhibits three crossovers at small, intermediate, and large scales; similar behavior is reported for DFA-1 in Fig. 6. Since both the crossover at small scales $n_{1\times}$ and the crossover at large scale $n_{3\times}$ result from the ''competition'' between the scaling of the correlated noise and the effect of the sinusoidal trend (Figs. 6 and 7), by using the superposition rule [Eq. (10)] we can estimate $n_{1\times}$ and $n_{3\times}$ as the intercepts of $F_\eta(n)$ and $F_S(n)$ for the general case of DFA-l.

For $n_{1\times}$ we find the following dependence on the period T, amplitude A_S, the correlation exponent α of the noise, and the order l of the DFA-l method:

$$n_{1\times}\sim(T/A_S)^{1/(l+1-\alpha)}. \tag{16}$$

For DFA-1, we have $l=1$ and we recover Eq. (14). In addi-

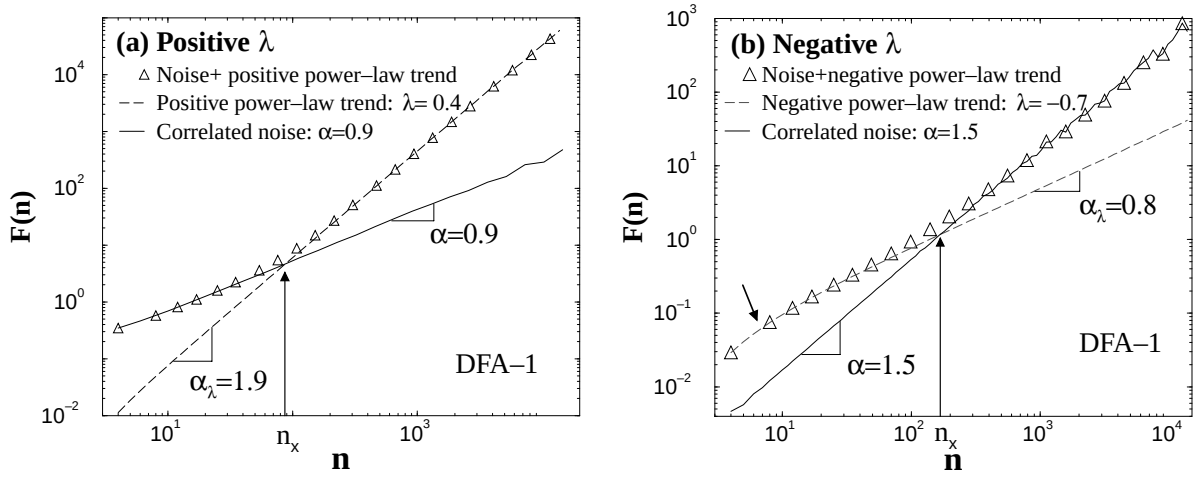

FIG. 10. Crossover behavior of the rms fluctuation function $F_{\eta P}(n)$ (circles) for correlated noise (of length $N_{max}=2^{17}$) with a superposed power-law trend $u(i)=A_{\mathrm{P}}i^{\lambda}$. The rms fluctuation function $F_{\eta}(n)$ for noise (solid line) and the rms fluctuation function $F_{\mathrm{P}}(n)$ (dashed line) are also shown for comparison. The DFA-1 method is used. (a) $F_{\eta P}(n)$ for noise with correlation exponent $\alpha_{\lambda}=0.9$ and the power-law trend with amplitude $A_{\mathrm{P}}=1000/(N_{max})^{0.4}$ and positive power $\lambda=0.4$. (b) $F_{\eta P}(n)$ for Brownian noise (integrated white noise, $\alpha_{\lambda}=1.5$) and the power-law trend with amplitude $A_{\mathrm{P}}=0.01/(N_{max})^{-0.7}$ and negative power $\lambda=-0.7$. Note that although in both cases there is a ''similar'' crossover behavior for $F_{\eta P}(n)$, the results in (a) and (b) represent completely opposite situations: while in (a) the power-law trend with positive power λ dominates the scaling of $F_{\eta P}(n)$ at large scales, in (b) the power-law trend with negative power λ dominates the scaling at small scales. The arrow in (b) indicates a weak crossover in $F_{\mathrm{P}}(n)$ (dashed lines) at small scales for negative power λ.

tion, $n_{1\times}$ is shifted to larger scales when higher-order DFA-l is applied, due to the fact that the value of $F_{\mathrm{S}}(n)$ decreases when l increases ($\alpha_{\mathrm{S}}=l+1$, see Fig. 9).

For the third crossover observed in $F_{\eta S}(n)$ at large scale $n_{3\times}$ we find for all orders l of the DFA-l the following scaling relation:

$$n_{3\times}\sim(TA_{\mathrm{S}})^{1/\alpha}. \tag{17}$$

Since the scaling function $F_{\eta}(n)$ for correlated noise shifts vertically to lower values when higher-order DFA-l is used (see the discussion in Appendix A and Sec. V B), $n_{3\times}$ exhibits a slight shift to larger scales.

For the crossover $n_{2\times}$ in $F_{\eta S}(n)$ at $F_{\eta S}(n)$ at intermediate scales, we find $n_{2\times}\sim T$. This relation is independent of the order l of the DFA and is identical to the relation found for $F_{\mathrm{S}}(n)$ [Eq. (11)]. $n_{2\times}$ also exhibits a shift to larger scales when higher-order DFA is used (see Fig. 9).

The features reported here of the crossovers in $F_{\eta S}(n)$ can be used to identify low-frequency sinusoidal trends in noisy data and to recognize their effects on the scaling properties of the data. This information may be useful when quantifying correlation properties in data by means of a scaling analysis.

V. NOISE WITH POWER-LAW TRENDS

In this section we study the effect of power-law trends on the scaling properties of noisy signals. We consider the case of correlated noise with a superposed power-law trend $u(i)=A_{\mathrm{P}}i^{\lambda}$, when A_{P} is a positive constant, $i=1,\ldots,N_{max}$, and N_{max} is the length of the signal. We find that when the DFA-1 method is used, the rms fluctuation function $F_{\eta P}(n)$ exhibits a crossover between two scaling regions (Fig. 10). This behavior results from the fact that at different scales n, either the correlated noise or the power-law trend is dominant, and can be predicted by employing the superposition rule

$$[F_{\eta P}(n)]^2=[F_{\eta}(n)]^2+[F_{\mathrm{P}}(n)]^2, \tag{18}$$

where $F_{\eta}(n)$ and $F_{\mathrm{P}}(n)$ are the rms fluctuation function of noise and the power-law trend, respectively, and $F_{\eta P}(n)$ is the rms fluctuation function for the superposition of the noise and the power-law trend. Since the behavior of $F_{\eta}(n)$ is known [Eq. (6) and Appendix A], we can understand the features of $F_{\eta P}(n)$ if we know how $F_{\mathrm{P}}(n)$ depends on the characteristics of the power-law trend. We note that the scaling behavior of $F_{\eta P}(n)$ displayed in Fig. 10(a) is to some extent similar to the behavior of the rms fluctuation function $F_{\eta L}(n)$ for correlated noise with a linear trend (Fig. 1)—e.g., the noise is dominant at small scales n, while the trend is dominant at large scales. However, the behavior $F_{\mathrm{P}}(n)$ is more complex than that of $F_{\mathrm{L}}(n)$ for the linear trend, since the effective exponent α_{λ} for $F_{\mathrm{P}}(n)$ can depend on the power λ of the power-law trend. In particular, for negative values of λ, $F_{\mathrm{P}}(n)$ can become dominated at small scales [Fig. 10(b)] while $F_{\eta}(n)$ dominates at large scales—a situation completely opposite of noise with a linear trend (Fig. 1) or with a power-law trend with positive values for the power λ. Moreover, $F_{\mathrm{P}}(n)$ can exhibit crossover behavior at small scales [Fig. 10(b)] for negative λ which is not observed for positive λ. In addition, $F_{\mathrm{P}}(n)$ depends on the order l of the DFA method and the length N_{max} of the signal. We discuss the scaling features of the power-law trends in the following three sections, V A–V C.

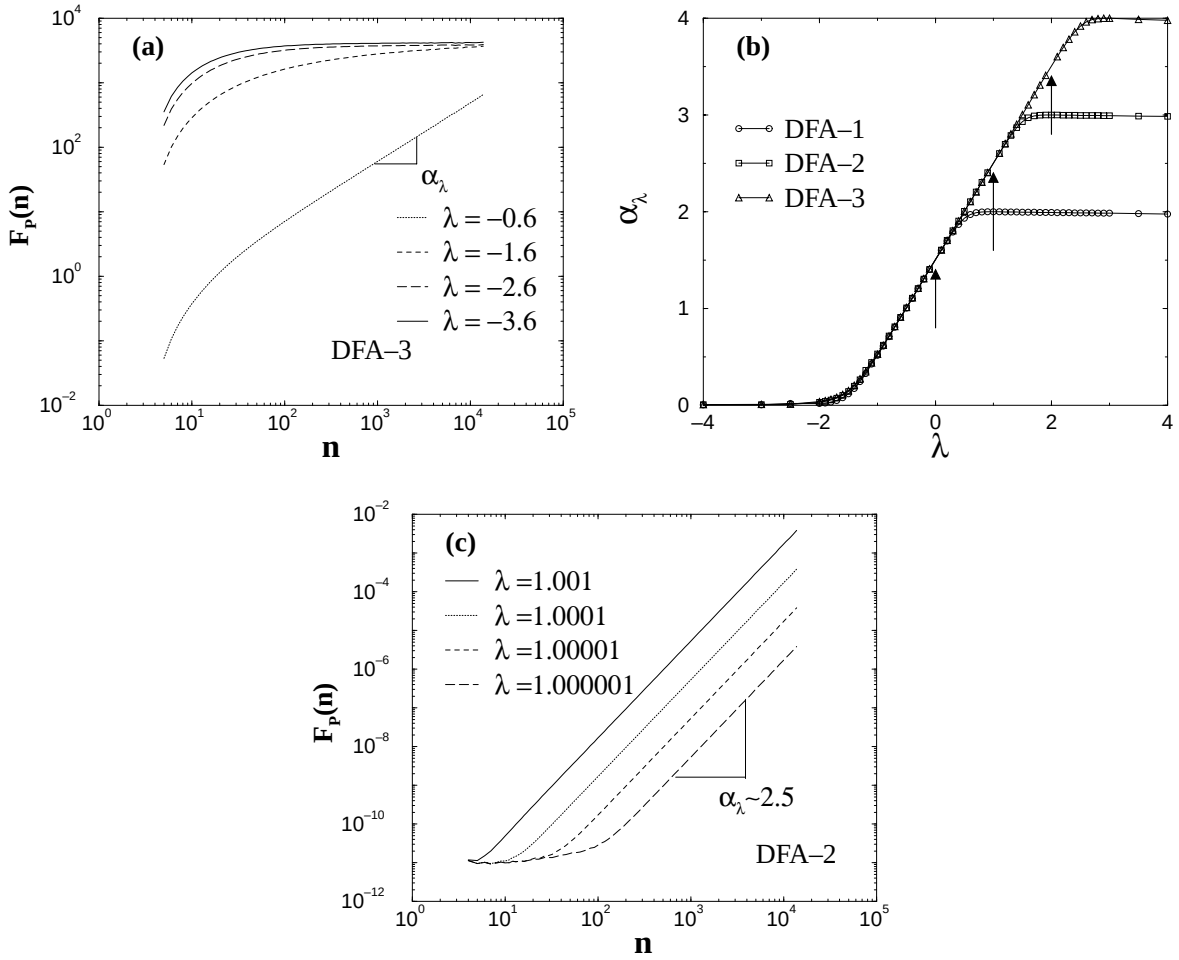

FIG. 11. Scaling behavior of the rms fluctuation function $F_P(n)$ for power-law trends, $u(i)\sim i^\lambda$, where $i=1,\ldots,N_{max}$ and $N_{max}=2^{17}$ is the length of the signal. (a) For $\lambda<0$, $F_P(n)$ exhibits crossover at small scales which is more pronounced with increasing the order l of DFA-l and decreasing the value of λ. Such crossover is not observed for $\lambda>0$ when $F_P(n)\sim n^{\alpha_\lambda}$ for all scales n [see Fig. 10(a)]. (b) Dependence of the effective exponent α_λ on the power λ for different order $l=1,2,3$ of the DFA method. Three regions are observed, depending on the order l of the DFA: region I ($\lambda>l-0.5$), where $\alpha_\lambda\approx l+1$; region II ($-1.5<\lambda<l-0.5$), where $\alpha_\lambda=\lambda+1.5$; region III ($\lambda<-1.5$), where $\alpha_\lambda\approx 0$. We note that for integer values of the power $\lambda=0,1,\ldots,l-1$, where l is the order of DFA we used, there is no scaling for $F_P(n)$ and α_λ is not defined, as indicated by the arrows. (c) Asymptotic behavior near integer values of λ. $F_P(n)$ is plotted for $\lambda\to 1$ when DFA-2 is used. Even for $\lambda-1=10^{-6}$, we observe at large scales n a region with an effective exponent $\alpha_\lambda\approx 2.5$. This region is shifted to infinitely large scales when $\lambda=1$.

A. Dependence of $F_P(n)$ on the power λ

First we study how the rms fluctuation function $F_P(n)$ for a power-law trend $u(i)=A_P i^\lambda$ depends on the power λ. We find that

$$F_P(n)\sim A_P n^{\alpha_\lambda}, \tag{19}$$

where α_λ is the effective exponent for the power-law trend. For positive λ we observe no crossovers in $F_P(n)$ [Fig. 10(a)]. However, for negative λ there is a crossover in $F_P(n)$ at small scales n [Fig. 10(b)], and we find that this crossover becomes even more pronounced with decreasing λ or increasing the order l of the DFA method, and is also shifted to larger scales [Fig. 11(a)].

Next, we study how the effective exponent α_λ for $F_P(n)$ depends on the value of the power λ for the power-law trend. We examine the scaling of $F_P(n)$ and estimate α_λ for $-4<\lambda<4$. In the cases when $F_P(n)$ exhibits a crossover, in order to obtain α_λ we fit the range of larger scales to the right of the crossover. We find that for any order l of the DFA-l method there are three regions with different relations between α_λ and λ [Fig. 11(b)]. They are as follows:

(i) $\alpha_\lambda\approx l+1$ for $\lambda>l-0.5$ (region I).

(ii) $\alpha_\lambda\approx\lambda+1.5$ for $-1.5\leqslant\lambda\leqslant l-0.5$ (region II).

(iii) $\alpha_\lambda\approx 0$ for $\lambda<-1.5$ (region III).

Note that for integer values of the power λ ($\lambda=0,1,\ldots,m-1$), i.e., polynomial trends of order $m-1$, the DFA-l method of order $l>m-1$ (l is also an integer) leads to $F_P(n)\approx 0$, since DFA-l is designed to remove polynomial trends. Thus for integer values of the power λ there is no scaling and the effective exponent α_λ is not defined if a DFA-l method of order $l>\lambda$ is used (Fig. 11). However, it is

of interest to examine the asymptotic behavior of the scaling of $F_{\rm P}(n)$ when the value of the power λ is close to an integer. In particular, we consider how the scaling of $F_{\rm P}(n)$ obtained from the DFA-2 method changes when $\lambda \to 1$ [Fig. 11(c)]. Surprisingly, we find that even though the values of $F_{\rm P}(n)$ are very small at large scales, there is a scaling for $F_{\rm P}(n)$ with a smooth convergence of the effective exponent $\alpha_\lambda \to 2.5$ when $\lambda \to 1$, according to the dependence $\alpha_\lambda \approx \lambda + 1.5$ established for region II [Fig. 11(b)]. At smaller scales there is a flat region which is due to the fact that the fluctuation function $Y(i)$ [Eq. (3)] is smaller than the precision of the numerical simulation.

B. Dependence of $F_{\rm P}(n)$ on the order l of DFA

Another factor that affects the rms fluctuation function of the power-law trend $F_{\rm P}(n)$ is the order l of the DFA method used. We first take into account the following.

(1) For integer values of the power λ, the power-law trend $u(i) = A_{\rm P} i^\lambda$ is a polynomial trend which can be perfectly filtered out by the DFA method of order $l > \lambda$, and as discussed in Secs. III B and V A [see Figs. 11(b) and 11(c)], there is no scaling for $F_{\rm P}(n)$. Therefore, in this section we consider only noninteger values of λ.

(2) For a given value of the power λ, the effective exponent α_λ can take different values depending on the order l of the DFA method we use (see Fig. 11)—e.g., for fixed $\lambda > l - 0.5, \alpha_\lambda \approx l + 1$. Therefore, in this section we consider only the case when $\lambda < l - 0.5$ (regions II and III).

Since higher-order DFA-l provides a better fit for the data, the fluctuation function $Y(i)$ [Eq. (3)] decreases with increasing order l. This leads to a vertical shift to smaller values of the rms fluctuation function $F(n)$ [Eq. (4)]. Such a vertical shift is observed for the rms fluctuation function $F_\eta(n)$ for correlated noise (see Appendix A), as well as for the rms fluctuation function of power-law trend $F_{\rm P}(n)$. Here we ask how this vertical shift in $F_\eta(n)$ and $F_{\rm P}(n)$ depends on the order l of the DFA method, and if this shift has different properties for $F_\eta(n)$ compared to $F_{\rm P}(n)$. This information can help identify power-law trends in noisy data, and can be used to differentiate crossovers separating scaling regions with different types of correlations and crossovers that are due to effects of power-law trends.

We consider correlated noise with a superposed power-law trend, where the crossover in $F_{\eta P}(n)$ at large scales n results from the dominant effect of the power-law trend—$F_{\eta P}(n) \approx F_{\rm P}(n)$ [Eq. (18) and Fig. 10(a)]. We choose the power $\lambda < 0.5$, a range where for all orders l of the DFA method the effective exponent α_λ of $F_{\rm P}(n)$ remains the same, i.e., $\alpha_\lambda = \lambda + 1.5$ [region II in Fig. 11(b)]. For a superposition of an anticorrelated noise and power-law trend with $\lambda = 0.4$, we observe a crossover in the scaling behavior of $F_{\eta P}(n)$, from a scaling region characterized by the correlation exponent $\alpha = 0.1$ of the noise, where $F_{\eta P}(n) \approx F_\eta(n)$, to a region characterized by an effective exponent $\alpha_\lambda = 1.9$, where $F_{\eta P}(n) \approx F_{\rm P}(n)$, for all orders $l = 1,2,3$ of the DFA-l method [Fig. 12(a)]. We also find that the crossover of $F_{\eta P}(n)$ shifts to larger scales when the order l of DFA-l increases, and that there is a vertical shift of $F_{\eta P}(n)$ to lower values. This vertical shift in $F_{\eta P}(n)$ at large scales, where $F_{\eta P}(n) = F_{\rm P}(n)$, appears to be different in magnitude when different order l of the DFA-l method is used [Fig. 12(a)]. We also observe a less pronounced vertical shift at small scales where $F_{\eta P}(n) \approx F_\eta(n)$.

Next, we ask how these vertical shifts depend on the order l of DFA-l. We define the vertical shift Δ as the y intercept of $F_{\rm P}(n)$: $\Delta \equiv F_{\rm P}(n=1)$. We find that the vertical shift Δ in $F_{\rm P}(n)$ for the power-law trend follows a power law: $\Delta \sim l^{\tau(\lambda)}$. We tested this relation for orders up to $l = 10$, and we find that it holds for different values of the power λ of the power-law trend [Fig. 12(b)]. Using Eq. (19) we can write $F_{\rm P}(n)/F_{\rm P}(n=1) = n^{\alpha_\lambda}$, i.e., $F_{\rm P}(n) \sim F_{\rm P}(n=1)$. Since $F_{\rm P}(n=1) \equiv \Delta \sim l^{\tau(\lambda)}$ [Fig. 12(b)], we find that

$$F_{\rm P}(n) \sim l^{\tau(\lambda)}. \tag{20}$$

We also find that the exponent τ is negative and is a decreasing function of the power λ [Fig. 12(c)]. Because the effective exponent α_λ which characterizes $F_{\rm P}(n)$ depends on the power λ [see Fig. 11(b)], we can express the exponent τ as a function of α_λ as we show in Fig. 12(d). This representation can help us compare the behavior of the vertical shift Δ in $F_{\rm P}(n)$ with the shift in $F_\eta(n)$. For correlated noise with a different correlation exponent α, we observe a similar power-law relation between the vertical shift in $F_\eta(n)$ and the order l of DFA-l: $\Delta \sim l^{\tau(\alpha)}$, where τ is also a negative exponent that decreases with α. In Fig. 12(d) we compare $\tau(\alpha_\lambda)$ for $F_{\rm P}(n)$ with $\tau(\alpha)$ for $F_\eta(n)$, and find that for any $\alpha_\lambda = \alpha$, $\tau(\alpha_\lambda) < \tau(\alpha)$. This difference between the vertical shift for correlated noise and for a power-law trend can be utilized to recognize effects of power-law trends on the scaling properties of data.

C. Dependence of $F_{\rm P}(n)$ on the signal length N_{max}

Here we study how the rms fluctuation function $F_{\rm P}(n)$ depends on the length N_{max} of the power-law signal $u(i) = A_{\rm P} i^\lambda$ $(i = 1, \ldots, N_{max})$. We find that there is a vertical shift in $F_{\rm P}(n)$ with increasing N_{max} [Fig. 13(a)]. We observe that when doubling the length N_{max} of the signal the vertical shift in $F_{\rm P}(n)$, which we define as $F_{\rm P}^{2N_{max}}/F_{\rm P}^{N_{max}}$, remains the same, independent of the value of N_{max}. This suggests a power-law dependence of $F_{\rm P}(n)$ on the length of the signal:

$$F_{\rm P}(n) \sim (N_{max})^\gamma, \tag{21}$$

where γ is an effective scaling exponent.

Next, we ask if the vertical shift depends on the power λ of the power-law trend. When doubling the length N_{max} of the signal, we find that for $\lambda < l - 0.5$, where l is the order of the DFA method, the vertical shift is a constant independent of λ [Fig. 13(b)]. Since the value of the vertical shift when doubling the length N_{max} is 2^γ [from Eq. (21)], the results in Fig. 13(b) show that γ is independent of λ when $\lambda < l - 0.5$, and that $-\log 2^\gamma \approx -0.15$, i.e. The effective exponent $\gamma \approx -0.5$.

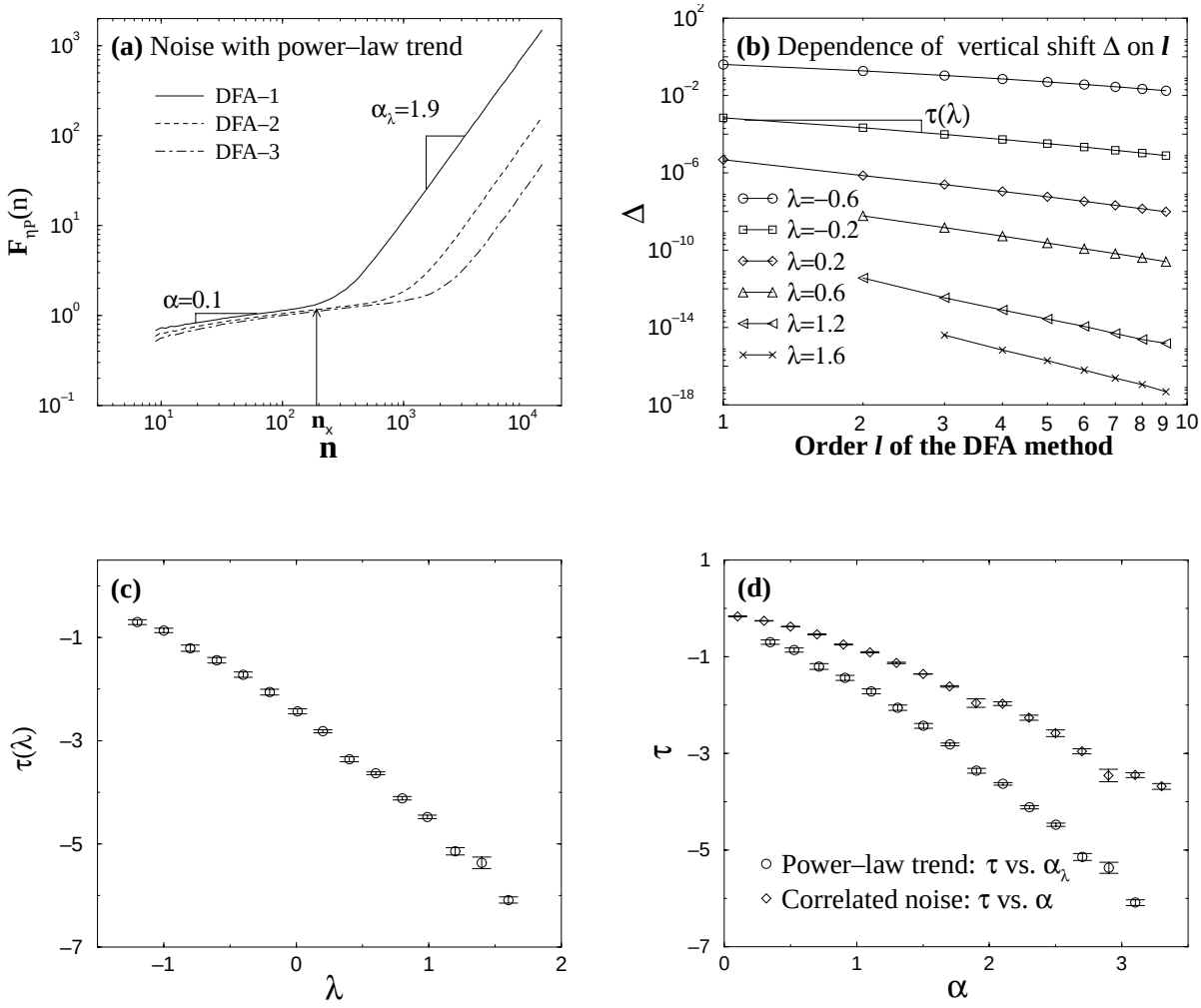

FIG. 12. Effect of higher-order DFA-l on the rms fluctuation function $F_{\eta P}(n)$ for correlated noise with a superposed power-law trend. (a) $F_{\eta P}(n)$ for anticorrelated noise with the correlation exponent $\alpha=0.1$ and a power-law $u(i)=A_{\mathrm{P}}i^{\lambda}$, where $A_{\mathrm{P}}=25/(N_{max})^{0.4}$, $N_{max}=2^{17}$, and $\lambda=0.4$. Results for different order $l=1,2,3$ of the DFA method show (i) a clear crossover from a region at small scales where the noise dominates $F_{\eta P}(n)\approx F_{\eta}(n)$ to a region at larger scales where the power-law trend dominates $F_{\eta P}(n)\approx F_{\mathrm{P}}(n)$, and (ii) a vertical shift Δ in $F_{\eta P}$ with increasing l. (b) Dependence of the vertical shift Δ in the rms fluctuation function $F_{\mathrm{P}}(n)$ for a power-law trend on the order l of DFA-l for different values of λ: $\Delta\sim l^{\tau(\lambda)}$. We define the vertical shift Δ as the y intercept of $F_{\mathrm{P}}(n)$: $\Delta\equiv F_{\mathrm{P}}(n=1)$. Note, that we consider only noninteger values for λ and that we consider the region $\lambda<l-0.5$. Thus, for all values of λ the minimal order l that can be used in the DFA method is $l>\lambda+0.5$, e.g., for $\lambda=1.6$ the minimal order of the DFA that can be used is $l=3$ [for details see Fig. 11(b)]. (c) Dependence of τ on the power λ [error bars indicate the regression error for the fits of $\Delta(l)$ in (b)]. (d) Comparison of $\tau(\alpha_{\lambda})$ for $F_{\mathrm{P}}(n)$ and $\tau(\alpha)$ for $F_{\eta}(n)$. Faster decay of $\tau(\alpha_{\lambda})$ indicates larger vertical shifts for $F_{\mathrm{P}}(n)$ compared to $F_{\eta}(n)$ with increasing order l of the DFA-l.

For $\lambda>l-0.5$, when doubling the length N_{max} of the signal, we find that the vertical shift 2^{γ} exhibits the following dependence on λ: $-\log_{10}2^{\gamma}=\log_{10}2^{\lambda-l}$, and thus the effective exponent γ depends on λ — $\gamma=\lambda-l$. For positive integer values of λ ($\lambda=l$), we find that $\gamma=0$, and there is no shift in $F_{\mathrm{P}}(n)$, suggesting that $F_{\mathrm{P}}(n)$ does not depend on the length N_{max} of the signal, when DFA of order l is used (Fig. 13). Finally, we note that depending on the effective exponent γ, i.e., on the order l of the DFA method and the value of the power λ, the vertical shift in the rms fluctuation function $F_{\mathrm{P}}(n)$ for the power-law trend can be positive ($\lambda>l$), negative ($\lambda<l$), or zero ($\lambda=l$).

D. Combined effect on $F_{\mathrm{P}}(n)$ of λ, l, and N_{max}

We have seen that by taking into account the effects of the power λ [Eq. (19)], the order l of DFA-l [Eq. (20)], and the effect of the length of the signal N_{max} [Eq. (21)], we reach the following expression for the rms fluctuation function $F_{\mathrm{P}}(n)$ for a power-law trend $u(i)=A_{\mathrm{P}}i^{\lambda}$:

$$F_{\mathrm{P}}(n)\sim A_{\mathrm{P}}n^{\alpha_{\lambda}}l^{\tau(\lambda)}(N_{max})^{\gamma(\lambda)}. \tag{22}$$

For correlated noise, the rms fluctuation function $F_{\eta}(n)$ de-

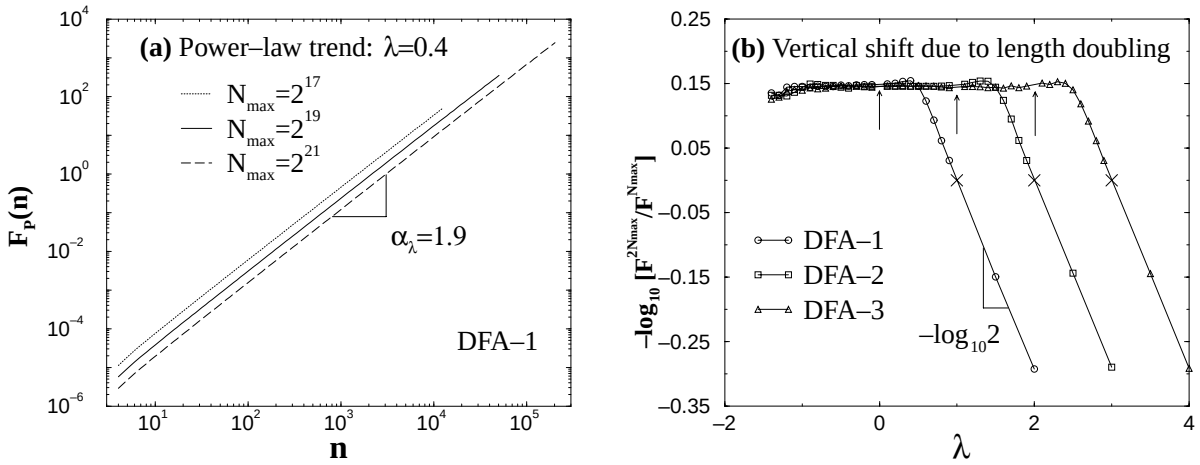

FIG. 13. Dependence of the rms fluctuation function $F_{\mathrm{P}}(n)$ for a power-law trend $u(i)=A_{\mathrm{P}}i^{\lambda}$, where $i=1,\ldots,N_{max}$, on the length of the trend N_{max}. (a) A vertical shift is observed in $F_{\mathrm{P}}(n)$ for different values of N_{max}—N_{1max} and N_{2max}. The figure shows that the vertical shift, defined as $F_{\mathrm{P}}^{N_{1max}}(n)/F_{\mathrm{P}}^{N_{2max}}(n)$, does not depend on N_{max} but only on the ratio N_{1max}/N_{2max}, suggesting that $F_{\mathrm{P}}(n)\sim(N_{max})^{\gamma}$. (b) Dependence of the vertical shift on the power λ. For $\lambda<l-0.5$ (l is the order of DFA), we find a flat (constant) region characterized with an effective exponent $\gamma=-0.5$ and negative vertical shift. For $\lambda>l-0.5$, we find an exponential dependence of the vertical shift on λ. In this region, $\gamma=\lambda-l$, and the vertical shift can be negative (if $\lambda<l$) or positive (if $\lambda>l$). The slope of $-\log_{10}[F_{\mathrm{P}}^{2N_{max}}(n)/F_{\mathrm{P}}^{N_{max}}(n)]$ vs λ is $-\log_{10}2$ due to doubling the length of the signal N_{max}. This slope changes to $-\log_{10}m$ when N_{max} is increased m times while γ remains independent of N_{max}. For $\lambda=l$ there is no vertical shift, as marked with $\times$. Arrows indicate integer values of $\lambda<l$, for which values the DFA-l method filters out completely the power-law trend and $F_{\mathrm{P}}=0$.

pends on the box size n [Eq. (6)] and on the order l of DFA-l [Sec. V B and Fig. 12(a), (d)], and does not depend on the length of the signal N_{max}. Thus we have the following expression for $F_{\eta}(n)$:

$$F_{\eta}(n)\sim n^{\alpha}l^{\tau(\alpha)}. \tag{23}$$

To estimate the crossover scale $n_{\times}$ observed in the apparent scaling of $F_{\eta P}(n)$ for a correlated noise superposed with a power-law trend [Figs. 10(a), 10(b), and 12(a)], we employ the superposition rule [Eq. (18)]. From Eqs. (22) and (23), we obtain $n_{\times}$ as the intercept between $F_{\mathrm{P}}(n)$ and $F_{\eta}(n)$,

$$n_{\times}\sim[Al^{\tau(\lambda)-\tau(\alpha)}(N_{max})^{\gamma}]^{1/(\alpha-\alpha_{\lambda})}. \tag{24}$$

To test the validity of this result, we consider the case of correlated noise with a linear trend. For the case of a linear trend ($\lambda=1$) when DFA-1 ($l=1$) is applied, we have $\alpha_{\lambda}=2$ [see Appendix C and Sec. V A, Fig. 11(b)]. Since in this case $\lambda=l=1>l-0.5$ we have $\gamma=\lambda-l=0$ [see Sec.V C, Fig. 13(b)], and from Eq. (24) we recover Eq. (9).

VI. CONCLUSION AND SUMMARY

In this paper we show that the DFA method performs better than the standard R/S analysis to quantify the scaling behavior of noisy signals for a wide range of correlations, and we estimate the range of scales where the performance of the DFA method is optimal. We consider different types of trends superposed on correlated noise, and we study how these trends affect the scaling behavior of the noise. We demonstrate that there is a competition between a trend and a noise, and that this competition can lead to crossovers in the scaling. We investigate the features of these crossovers, their dependence on the properties of the noise, and the superposed trend. Surprisingly, we find that crossovers which are a result of trends can exhibit power-law dependences on the parameters of the trends. We show that these crossover phenomena can be explained by the superposition of the separate results of the DFA method on the noise and on the trend, assuming that the noise and the trend are not correlated, and that the scaling properties of the noise and the apparent scaling behavior of the trend are known. Our work may provide some help to differentiate between different types of crossovers, e.g., crossovers that separate scaling regions with different correlation properties may differ from crossovers that are an artifact of trends. The results we present here could be useful for identifying the presence of trends and to accurately interpret correlation properties of noisy data. Related work on trends [64] and other forms of nonstationarity [65] will be published separately.

ACKNOWLEDGMENTS

We thank NIH/National Center for Research Resources (Grant No. P41RR13622), NSF, and the Spanish Government (Grant No. BIO99-0651-CO2-01) for support, and also A. L. Goldberger, C.-K. Peng, and Y. Ashkenazy for helpful discussions.

APPENDIX A: NOISE

The standard signals we generate in our study are uncorrelated, correlated, and anticorrelated noise. First we must have a clear idea of the scaling behaviors of these standard signals before we use them to study the effects from other

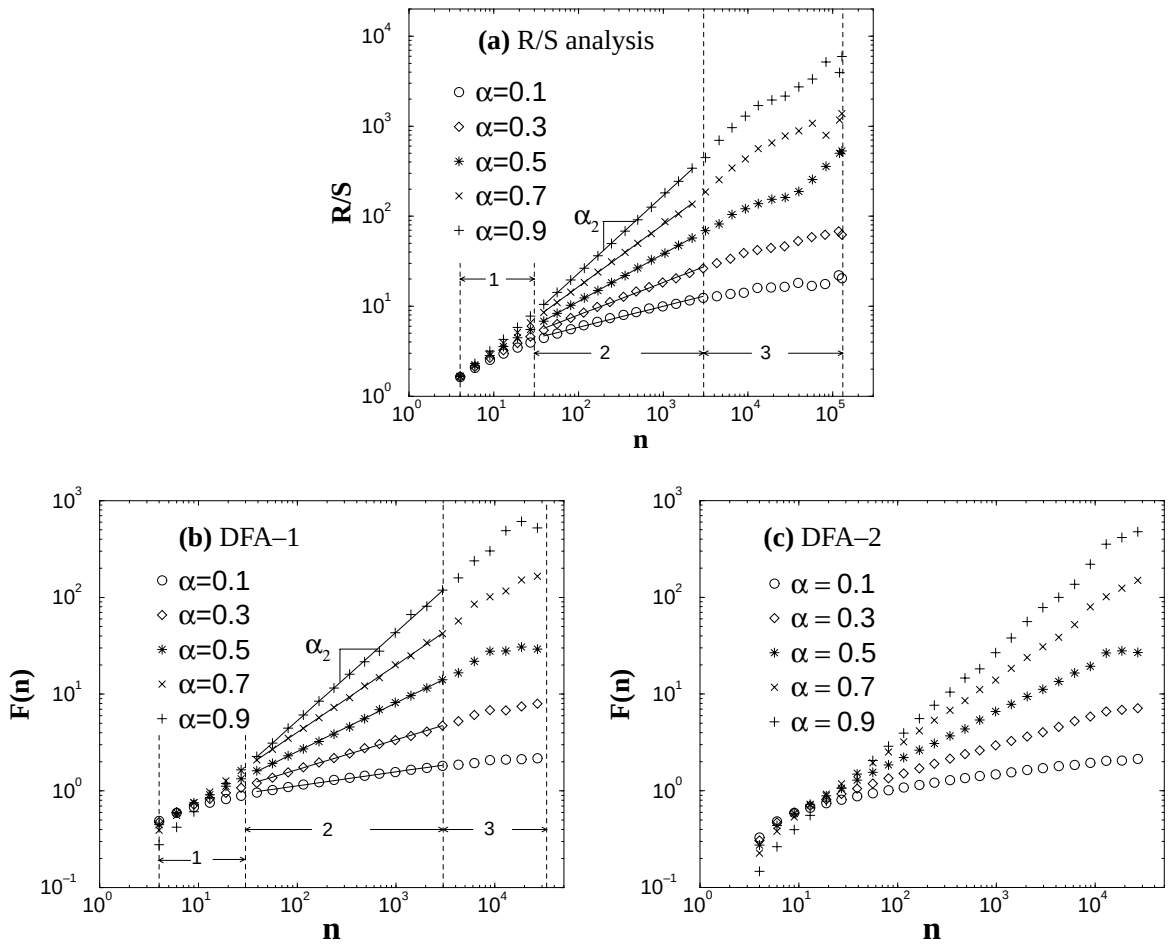

FIG. 14. Scaling behavior of noise with the scaling exponent α. The length of noise $N_{\max}=2^{17}$. (a) Rescaled range analysis (R/S). (b) Order-1 detrended fluctuation analysis (DFA-1). (c) Order-2 detrended fluctuation analysis (DFA-2). We do the linear fitting for the R/S analysis and the DFA-1 in three regions as shown and get α_1, α_2, and α_3 for estimated α, which are listed in Tables IV and V. We find that the estimation of α is different in the different regions.

aspects. We generate noises by using a modified Fourier filtering method [63]. This method can efficiently generate noise $u(i)$ $(i=1,2,3,\ldots,N_{\max})$, with the desired power-law correlation function that asymptotically behaves as $\langle|\Sigma_{j=i}^{i+t}u(j)|^2\rangle\sim t^{2\alpha}$. By default, a generated noise has standard deviation $\sigma=1$. Then we can test DFA and R/S by applying it on generated noises since we know the expected scaling exponent α.

Before doing that, we want to briefly review the algorithm of R/S analysis. For a signal $u(i)$ $(i=1,\ldots,N_{\max})$, it is divided into boxes of equal size n. In each box, the *cumulative departure* X_i (for the kth box, $i=kn+1,\ldots,kn+n$) is calculated

$$X_i=\sum_{j=kn+1}^{i}[u(j)-\langle u\rangle], \tag{A1}$$

where $\langle u\rangle=n^{-1}\Sigma_{i=kn+1}^{(k+1)n}u(i)$, and the *rescaled range* R/S is defined by

$$R/S=S^{-1}\left[\max_{kn+1\le i\le(k+1)n}X_i-\min_{kn+1\le i\le(k+1)n}X_i\right], \tag{A2}$$

where $S=\sqrt{n^{-1}\Sigma_{j=1}^{n}[u(j)-\langle u\rangle]^2}$ is the standard deviation in each box. The average of rescaled range in all the boxes of equal size n, is obtained and denoted by $\langle R/S\rangle$. Repeat the above computation over different box size n to provide a relationship between $\langle R/S\rangle$ and n. According to Hurst's experimental study [66], a power-law relation between $\langle R/S\rangle$ and the box size n indicates the presence of scaling: $\langle R/S\rangle\sim n^{\alpha}$.

Figure 14 shows the results of R/S, DFA-1, and DFA-2 on the same generated noises. Loosely speaking, we can see that $F(n)$ (for DFA) and R/S (for R/S analysis) show a power-law relation with n as expected: $F(n)\sim n^{\alpha}$ and $R/S\sim n^{\alpha}$. In addition, there is no significant difference between the results of different order DFA except for some vertical shift of the curves and the little bend-down for small box size n. The bend-down for a very small box of $F(n)$ from higher-order DFA is because there are more variables to fit those few points.

Ideally, when analyzing a standard noise, $F(n)$ (DFA) and R/S (R/S analysis) will be power-law functions with a given power: α, no matter which region of $F(n)$ and R/S is

TABLE IV. Estimation of the correlation exponent α for correlated noise from the R/S analysis in three regions as shown in Fig. 14(a). α is the input value of the scaling exponent, α_1 is the estimation from region 1 ($4<n\leqslant 32$), α_2 from region 2 ($32<n\leqslant 3162$), and α_3 from region 3 ($3126<n\leqslant 2^{17}$). The same correlated noise is used in Table V.

α	α_1	α_2	α_3
0.1	0.44	0.23	0.12
0.3	0.52	0.37	0.23
0.5	0.62	0.52	0.47
0.7	0.72	0.70	0.45
0.9	0.81	0.87	0.63

TABLE V. Estimation of the correlation exponent α for correlated noise from DFA-1 in the three regions as shown in Fig. 14(b). α is the input value of the scaling exponent, α_1 is the estimation from region 1 ($4<n\leqslant 32$), α_2 from region 2 ($32<n\leqslant 3162$), and α_3 from region 3 ($3126<n\leqslant 2^{17}$).

α	α_1	α_2	α_3
0.1	0.28	0.15	0.08
0.3	0.40	0.31	0.22
0.5	0.55	0.50	0.35
0.7	0.72	0.69	0.55
0.9	0.91	0.91	0.69

chosen. However, a careful study shows that the scaling exponent α depends on scale n. The estimated α is different for the different regions of $F(n)$ and R/S as illustrated by Figs. 14(a) and 14(b) and by Tables IV and V. It is very important to know the best fitting region of the DFA and R/S analysis in the study of real signals. Otherwise, an inaccurate value for α will be obtained if an inappropriate region is selected.

In order to find the best region, we first determine the dependence of the locally estimated α, $\alpha_{\rm loc}$, on the scale n. First, generate a standard noise with given scaling exponent

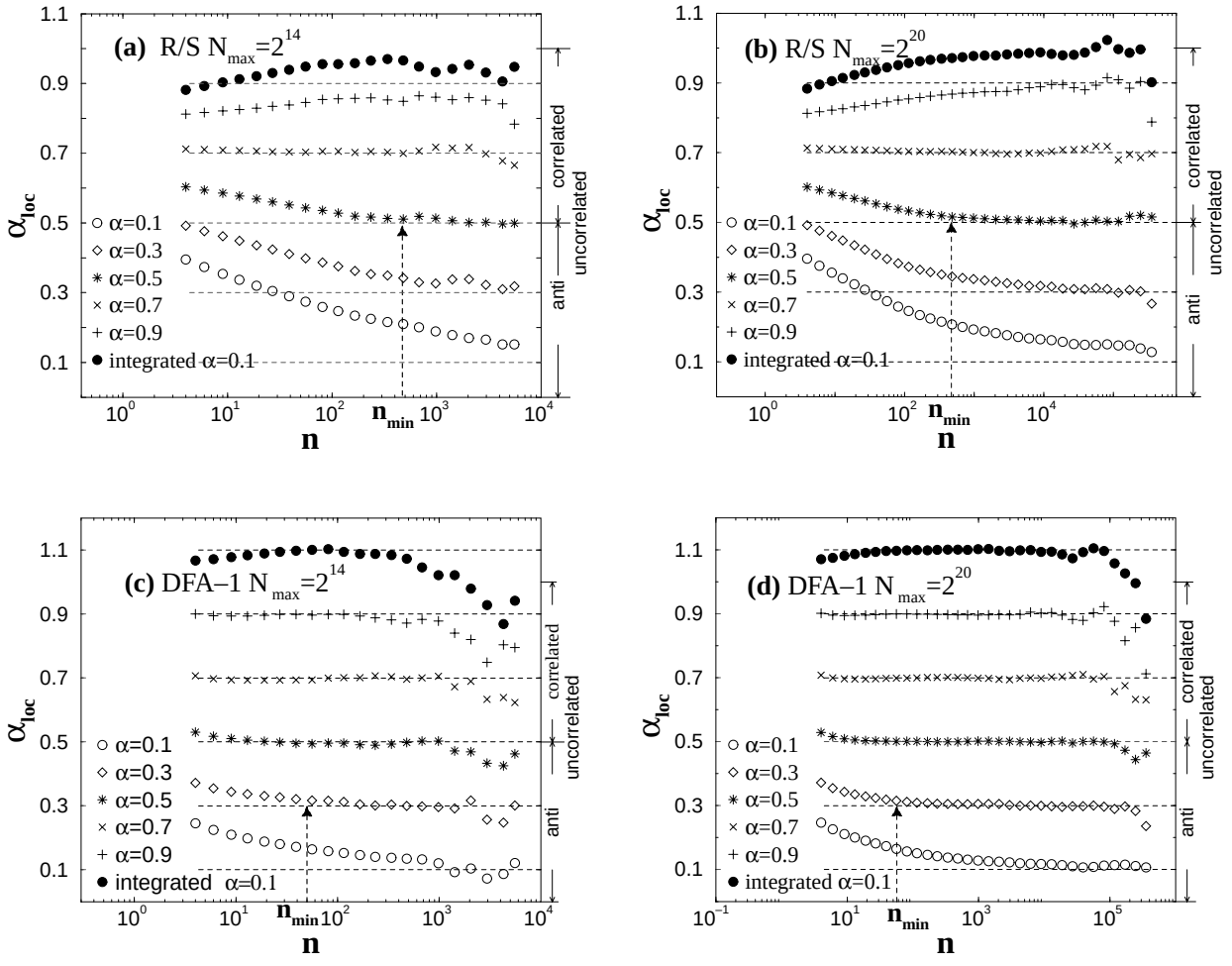

FIG. 15. The estimated α from the local fit (a) R/S analysis, the length of signal $N_{\rm max}=2^{14}$. (b) R/S analysis, $N_{\rm max}=2^{20}$. (c) DFA-1, $N_{\rm max}=2^{14}$. (d) DFA-1, $N_{\rm max}=2^{20}$. $\alpha_{\rm loc}$ come from the average of 50 simulations. If a technique is working, then the data for the scaling exponent α should be a weakly fluctuating horizontal line centered about $\alpha_{\rm loc}=\alpha$. Note that such a horizontal behavior does not hold for all the scales. Generally, such an expected behavior begins from some scale $n_{\rm min}$, holds for a range, and ends at a larger scale $n_{\rm max}$. For DFA-1, $n_{\rm min}$ is quite small $\alpha>0.5$. For the R/S analysis, $n_{\rm min}$ is quite small only when $\alpha\approx 0.7$.

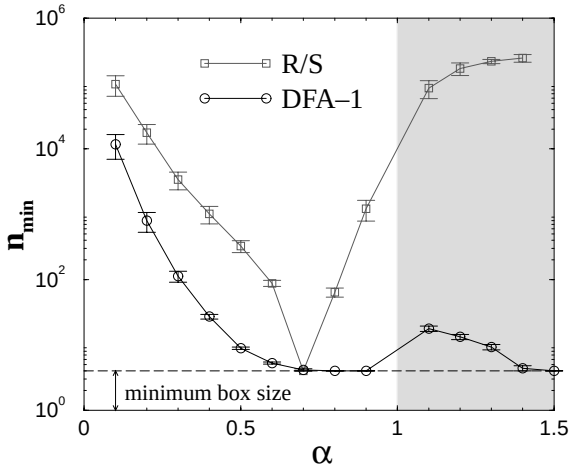

FIG. 16. The starting point of a good-fit region, $n_{\min}$, for the DFA-1 and R/S analyses. The results are obtained from 50 simulations, in which the length of noise is $N_{\max}=2^{20}$. The condition for a good fit is $\Delta\alpha=|\alpha_{\rm loc}-\alpha|<0.01$. The data for $\alpha>1.0$ shown in the shading area are obtained by applying an analysis on the integrations of noises with $\alpha<1.0$. It is clear that the DFA-1 works better than the R/S analysis because its $n_{\min}$ is always smaller than that of the R/S analysis.

α; then calculate $F(n)$ (or R/S), and obtain $\alpha_{\rm loc}(n)$ by local fitting of $F(n)$ (or R/S). The same random simulation is repeated 50 times for both the DFA and R/S analyses. The resultant average $\alpha_{\rm loc}(n)$, respectively, is illustrated in Fig. 15 for the DFA-1 and R/S analyses.

If a scaling analysis method is working properly, then the result $\alpha_{\rm loc}(n)$ from simulation with α would be a horizontal line with a slight fluctuation centered about $\alpha_{\rm loc}(n)=\alpha$. Note from Fig. 15 that such a *horizontal behavior* does not hold for all the scales n but for a certain range from $n_{\min}$ to $n_{\max}$. In addition, at small scale, the R/S analysis gives $\alpha_{\rm loc}>\alpha$ if $\alpha<0.7$ and $\alpha_{\rm loc}<\alpha$ if $\alpha>0.7$, which has been pointed out by Mandelbrot [67], while DFA gives $\alpha_{\rm loc}>\alpha$ if $\alpha<1.0$ and $\alpha_{\rm loc}<\alpha$ if $\alpha>1.0$.

It is clear that the smaller the $n_{\min}$ and the larger the $n_{\max}$, the better the method. We also perceive that the expected *horizontal behavior* stops because the fluctuations become larger due to the undersampling of $F(n)$ or R/S when n gets closer to the length of the signal $N_{\max}$. Furthermore, it can be seen from Fig. 15 that $n_{\max}\approx\frac{1}{10}N_{\max}$ independent of α (if the best-fit region exists), which is why one-tenth of the signal length can be considered as the maximum box size when using a DFA or R/S analysis.

On the contrary, $n_{\min}$ does not depend on the $N_{\max}$ since $\alpha_{\rm loc}(n)$ at small n hardly changes as $N_{\max}$ varies but it does depend on α. Thus, we obtain $n_{\min}$ quantitatively as shown in Fig. 16. For the R/S analysis, $n_{\min}$ is small only when $\alpha\approx0.7$. When $\alpha>0.7$ and $\alpha<0.7$, $n_{\min}$ becomes very large and close to $n_{\max}$, indicating that the best-fit region will vanish and the R/S analysis does not work at all.

Compared to R/S, DFA works better since $n_{\min}$ is quite small for correlated signals with $\alpha>0.5$. However, for $\alpha<0.5$ $n_{\min}$ is still relatively large. We can improve this situation by first integrating the correlated noise and then applying the DFA to the integrated signal. The resultant exponent α' for the integrated signal will be $\alpha_0'=\alpha+1$. We find that $n_{\min}$ for the integrated signal becomes much smaller as shown in Fig. 16 (shaded area $\alpha>1$). Therefore, for correlated noise with $\alpha<0.5$, it is best to estimate first the scaling exponent α' of the integrated signal and then to obtain α by $\alpha=\alpha'-1$.

APPENDIX B: SUPERPOSITION LAW FOR THE DFA

For two uncorrelated signals $f(i)$ and $g(i)$, their root-mean-square (rms) fluctuation functions are $F_f(n)$ and $F_g(n)$, respectively. We want to prove that for the signal $f(i)+g(i)$, its rms fluctuation function

$$F_{f+g}(n)=\sqrt{F_f(n)^2+F_g(n)^2}. \tag{B1}$$

Consider three signals in the same box first. The integrated signals for f, g, and $f+g$ are $y_f(i)$, $y_g(i)$, and $y_{f+g}(i)$ and their corresponding trends are y_f^{fit}, y_g^{fit}, and y_{f+g}^{fit} ($i=1,2,\ldots,n$, n is the box size). Since $y_{f+g}(i)=y_f(i)+y_g(i)$ and combines the definition of the detrended fluctuation function Eq. (3), we have that for all boxes

$$Y_{f+g}(i)=Y_f(i)+Y_g(i), \tag{B2}$$

where Y_{f+g} is the detrended fluctuation function for the signal $f+g$, $Y_f(i)$ is for the signal f, and $Y_g(i)$ for g. Furthermore, according to the definition of the rms fluctuation, we can obtain

$$\begin{aligned} F_{f+g}(n)&=\sqrt{\frac{1}{N_{max}}\sum_{i=1}^{N_{max}}[Y_{f+g}(i)]^2}\\ &=\sqrt{\frac{1}{N_{max}}\sum_{i=1}^{N_{max}}[Y_f(i)+Y_g(i)]^2}, \end{aligned} \tag{B3}$$

where l is the number of boxes and k means the kth box. If f and g are not correlated, neither are $Y_f(i)$ and $Y_g(i)$ and, thus,

$$\sum_{i=1}^{N_{max}}Y_f(i)Y_g(i)=0. \tag{B4}$$

From Eq. (B4) and Eq. (B3) we have

$$\begin{aligned} F_{f+g}(n)&=\sqrt{\frac{1}{N_{max}}\sum_{i=1}^{N_{max}}[Y_f(i)^2+Y_g(i)^2]}\\ &=\sqrt{[F_f(n)]^2+[F_g(n)]^2}. \end{aligned} \tag{B5}$$

APPENDIX C: DFA-1 ON LINEAR TREND

Let us suppose a linear time series $u(i)=A_{\rm L}i$. The integrated signal $y_L(i)$ is

$$y_L(i)=\sum_{j=1}^{i} A_{\mathrm{L}} j = A_{\mathrm{L}} \frac{i^2+i}{2}. \tag{C1}$$

Let as call N_{max} the size of the series and n the size of the box. The rms fluctuation $F_{\mathrm{L}}(n)$ as a function of n and N_{max} is

$$F_{\mathrm{L}}(n) = A_{\mathrm{L}} \sqrt{\frac{1}{N_{max}} \sum_{k=1}^{N_{max}/n} \sum_{i=(k-1)n+1}^{kn} \left(\frac{i^2+i}{2} - (a_k + b_k i) \right)^2}, \tag{C2}$$

where a_k and b_k are the parameters of a least-squares fit of the kth box of size n. a_k and b_k can be determined analytically, thus giving

$$a_k = 1 - \tfrac{1}{12} n^2 + \tfrac{1}{2} n^2 k + \tfrac{1}{12} n - \tfrac{1}{2} k^2 n^2, \tag{C3}$$

$$b_k = 1 - \tfrac{1}{2} n + kn + \tfrac{1}{2}. \tag{C4}$$

With these values, $F_{\mathrm{L}}(n)$ can be evaluated analytically,

$$F_{\mathrm{L}}(n) = A_{\mathrm{L}} \tfrac{1}{60} \sqrt{(5n^4 + 25n^3 + 25n^2 - 25n - 30)} \tag{C5}$$

The dominating term inside the square root is $5n^4$ and then one obtains

$$F_{\mathrm{L}}(n) \approx \frac{\sqrt{5}}{60} A_{\mathrm{L}} n^2, \tag{C6}$$

leading directly to an exponent of 2 in the DFA. An important consequence is that as $F(n)$ does not depend on N_{max}, for linear trends with the same slope, the DFA must give exactly the same results for series of different sizes. This is not true for other trends, where the exponent is 2, but the factor multiplying n^2 can depend on N_{max}.

APPENDIX D: DFA-1 ON A QUADRATIC TREND

Let us suppose now a series of the type $u(i)=A_{\mathrm{Q}} i^2$. The integrated time series $y(i)$ is

$$y(i) = A_{\mathrm{Q}} \sum_{j=1}^{i} j^2 = A_{\mathrm{Q}} \frac{2i^3 + 3i^2 + i}{6}. \tag{D1}$$

As before, let us call N_{max} and n the sizes of the series and box, respectively. The rms fluctuation function $F_{\mathrm{Q}}(n)$ measuring the rms fluctuation is now defined as

$$F_{\mathrm{Q}}(n) = A_{\mathrm{Q}} \sqrt{\frac{1}{N_{max}} \sum_{k=1}^{N_{max}/n} \sum_{i=(k-1)n+1}^{kn} \left(\frac{2i^3 + 3i^2 + i}{6} - (a_k + b_k i) \right)^2}, \tag{D2}$$

where a_k and b_k are the parameters of a least-squares fit of the kth box of size n. As before, a_k and b_k can be determined analytically, thus giving

$$a_k = \tfrac{1}{15} n^3 + n^3 k^2 - \tfrac{7}{15} n^3 k + \tfrac{17}{30} n^2 k - \tfrac{7}{60} n^2 + \tfrac{1}{20} n - \tfrac{2}{3} k^3 n^3 - \tfrac{1}{2} n^2 k^2 + \tfrac{1}{15} kn, \tag{D3}$$

$$b_k = \tfrac{3}{10} n^2 + n^2 k^2 - n^2 k + kn - \tfrac{2}{5} n + \tfrac{1}{10}. \tag{D4}$$

Once a_k and b_k are known, $F(n)$ can be evaluated, giving

$$F_{\mathrm{Q}}(n) = A_{\mathrm{Q}} \frac{1}{1260} \sqrt{-21(n^4 + 5n^3 + 5n^2 - 5n - 6)(32n^2 - 6n - 81 - 210N_{max} - 140N_{max}^2)}. \tag{D5}$$

As $N_{max} > n$, the dominant term inside the square root is given by $140N_{max}^2 \times 21n^4 = A_{\mathrm{Q}} 2940 n^4 N_{max}^2$, and then one has approximately

$$F_{\mathrm{Q}}(n) \approx A_{\mathrm{Q}} \tfrac{1}{1260} \sqrt{2940 n^4 N_{max}^2} = A_{\mathrm{Q}} \tfrac{1}{90} \sqrt{15} N_{max} n^2 \tag{D6}$$

leading directly to an exponent 2 in the DFA analysis. An interesting consequence derived from Eq. (D6) is that $F_{\mathrm{Q}}(n)$ depends on the length of the signal N_{max}, and the DFA line [$\log F_{\mathrm{Q}}(n)$ vs $\log n$] for the quadratic series $u(i)=A_{\mathrm{Q}} i^2$ of different N_{max} does not overlap (as is the case for linear trends).

[1] C.-K. Peng, S. V. Buldyrev, S. Havlin, M. Simons, H. E. Stanley, and A. L. Goldberger, Phys. Rev. E **49**, 1685 (1994).

[2] S. V. Buldyrev, A. L. Goldberger, S. Havlin, C.-K. Peng, H. E. Stanley, and M. Simons, Biophys. J. **65**, 2673 (1993).

[3] S. M. Ossadnik, S. B. Buldyrev, A. L. Goldberger, S. Havlin, R. N. Mantegna, C.-K. Peng, M. Simons, and H. E. Stanley, Biophys. J. **67**, 64 (1994).

[4] M. S. Taqqu, V. Teverovsky, and W. Willinger, Fractals **3**, 785 (1995).

[5] N. Iyengar, C.-K. Peng, R. Morin, A. L. Goldberger, and L. A.

Lipsitz, Am. J. Physiol. **40**, R1078 (1996).
[6] P. Ch. Ivanov, M. G. Rosenblum, C.-K. Peng, J. E. Mietus, S. Havlin, H. E. Stanley, and A. L. Goldberger, Nature (London) **383**, 323 (1996).
[7] K. K. L. Ho, G. B. Moody, C.-K. Peng, J. E. Mietus, M. G. Larson, D. Levy, and A. L. Goldberger, Circulation **96**, 842 (1997).
[8] P. Ch. Ivanov, M. G. Rosenblum, C.-K. Peng, J. E. Mietus, S. Havlin, H. E. Stanley, and A. L. Goldberger, Physica A **249**, 587 (1998).
[9] M. Barbi, S. Chillemi, A. Di Garbo, R. Balocchi, C. Carpeggiani, M. Emdin, C. Michelassi, and E. Santarcangelo, Chaos, Solitons Fractals **9**, 507 (1998).
[10] P. Ch. Ivanov, A. Bunde, L. A. Nunes Amaral, S. Havlin, J. Fritsch-Yelle, R. M. Baevsky, H. E. Stanley, and A. L. Goldberger, Europhys. Lett. **48**, 594 (1999).
[11] S. M. Pikkujamsa, T. H. Makikallio, L. B. Sourander, I. J. Raiha, P. Puukka, J. Skytta, C.-K. Peng, A. L. Goldberger, and H. V. Huikuri, Circulation **100**, 393 (1999).
[12] S. Havlin, S. V. Buldyrev, A. Bunde, A. L. Goldberger, P. Ch. Ivanov, C.-K. Peng, and H. E. Stanley, Physica A **273**, 46 (1999).
[13] H. E. Stanley, L. Amaral, A. L. Goldberger, S. Havlin, P. C. Ivanov, and C.-K. Peng, Physica A **270**, 309 (1999).
[14] Y. Ashkenazy, M. Lewkowicz, J. Levitan, S. Havlin, K. Saermark, H. Moelgaard, and P. E. B. Thomsen, Fractals **7**, 85 (1999).
[15] T. H. Makikallio, J. Koistinen, L. Jordaens, M. P. Tulppo, N. Wood, B. Golosarsky, C.-K. Peng, A. L. Goldberger, and H. V. Huikuri, Am. J. Cardiol. **83**, 880 (1999).
[16] C.-K. Peng, S. Havlin, H. E. Stanley, and A. L. Goldberger, Chaos **5**, 82 (1995).
[17] S. Havlin, S. V. Buldyrev, A. L. Goldberger, S. M. Ossadniksm, C.-K. Peng, M. Simons, and H. E. Stanley, Chaos, Solitons Fractals **6**, 171 (1995).
[18] P. A. Absil, R. Sepulchre, A. Bilge, and P. Gerard, Physica A **272**, 235 (1999).
[19] S. Havlin, L. A. Nunes Amaral, A. L. Goldberger, P. Ch. Ivanov, C.-K. Peng, and H. E. Stanley, Physica A **274**, 99 (1999).
[20] D. Toweill, K. Sonnenthal, B. Kimberly, S. Lai, and B. Goldstein, Crit. Care Med. **28**, 2051 (2000).
[21] A. Bunde, S. Havlin, J. W. Kantelhardt, T. Penzel, J. H. Peter, and K. Voigt, Phys. Rev. Lett. **85**, 3736 (2000).
[22] T. T. Laitio, H. V. Huikuri, E. S. H. Kentala, T. H. Makikallio, J. R. Jalonen, H. Helenius, K. Sariola-Heinonen, S. Yli-Mayry, and H. Scheinin, Anesthesiology **93**, 69 (2000).
[23] Y. Ashkenazy, P. Ch. Ivanov, S. Havlin, C.-K. Peng, A. L. Goldberger, and H. E. Stanley, Phys. Rev. Lett. **86**, 1900 (2001).
[24] C.-K. Peng, S. V. Buldyrev, A. L. Goldberger, S. Havlin, M. Simons, and H. E. Stanley, Phys. Rev. E **47**, 3730 (1993).
[25] H. E. Stanley, S. V. Buldyrev, A. L. Goldberger, S. Havlin, R. N. Mantegna, C.-K. Peng, and M. Simons, Nuovo Cimento D **16**, 1339 (1994).
[26] R. N. Mantegna, S. V. Buldyrev, A. L. Goldberger, S. Havlin, C.-K. Peng, M. Simons, and H. E. Stanley, Phys. Rev. Lett. **73**, 3169 (1994).
[27] C.-K. Peng, S. V. Buldyrev, A. L. Goldberger, S. Havlin, R. N. Mantegna, M. Simons, and H. E. Stanley, Physica A **221**, 180 (1995).
[28] S. Havlin, S. V. Buldyrev, A. L. Goldberger, R. N. Mantegna, C.-K. Peng, M. Simons, and H. E. Stanley, Fractals **3**, 269 (1995).
[29] R. N. Mantegna, S. V. Buldyrev, A. L. Goldberger, S. Havlin, C.-K. Peng, M. Simons, and H. E. Stanley, Phys. Rev. Lett. **76**, 1979 (1996).
[30] S. V. Buldyrev, N. V. Dokholyan, A. L. Goldberger, S. Havlin, C.-K. Peng, H. E. Stanley, and G. M. Viswanathan, Physica A **249**, 430 (1998).
[31] S. Blesic, S. Milosevic, D. Stratimirovic, and M. Ljubisavljevic, Physica A **268**, 275 (1999).
[32] H. Yoshinaga, S. Miyazima, and S. Mitake, Physica A **280**, 582 (2000).
[33] C. A. Perazzo, E. A. Fernandez, D. R. Chialvo, and P.l. Willshaw, Fractals **8**, 279 (2000).
[34] Z. Siwy, S. Mercik, K. Ivanova, and M. Ausloos, Physica A (to be published).
[35] Y. Liu, P. Cizeau, M. Meyer, C.-K. Peng, and H. E. Stanley, Physica A **245**, 437 (1997).
[36] N. Vandewalle and M. Ausloos, Physica A **246**, 454 (1997).
[37] N. Vandewalle and M. Ausloos, Phys. Rev. E **58**, 6832 (1998).
[38] Y. Liu, P. Gopikrishnan, P. Cizeau, M. Meyer, C.-K. Peng, and H. E. Stanley, Phys. Rev. E **60**, 1390 (1999).
[39] I. M. Janosi, B. Janecsko, and I. Kondor, Physica A **269**, 111 (1999).
[40] M. Ausloos, N. Vandewalle, P. Boveroux, A. Minguet, and K. Ivanova, Physica A **274**, 229 (1999).
[41] M. Roberto, E. Scalas, G. Cuniberti, and M. Riani, Physica A **269**, 148 (1999).
[42] N. Vandewalle, M. Ausloos, and P. Boveroux, Physica A **269**, 170 (1999).
[43] P. Grau-Carles, Physica A **287**, 396 (2000).
[44] M. Ausloos, Physica A **285**, 48 (2000).
[45] M. Ausloos and K. Ivanova, Physica A **286**, 353 (2000).
[46] M. Ausloos and K. Ivanova, Phys. Rev. E **63**, 047201 (2001).
[47] M. Ausloos and K. Ivanova, Int. J. Mod. Phys. C (to be published).
[48] K. Ivanova and M. Ausloos, Physica A **274**, 349 (1999).
[49] A. Montanari, R. Rosso, and M. S. Taqqu, Water Resour. Res. **36,** (5), 1249 (2000).
[50] C. Matsoukas, S. Islam, and I. Rodriguez-Iturbe, J. Geophys. Res., [Atmos.] **105**, 29 165 (2000).
[51] J. W. Kantelhardt, R. Berkovits, S. Havlin, and A. Bunde, Physica A **266**, 461 (1999).
[52] C. L. Alados and M. A. Huffman, Ethology **106**, 105 (2000).
[53] C.-K. Peng, J. E. Mietus, J. M. Hausdorff, S. Havlin, H. E. Stanley, and A. L. Goldberger, Phys. Rev. Lett. **70**, 1343 (1993).
[54] N. Makarenko, L. M. Karimova, B. I. Demchenko, and M. M. Novak, Fractals **6**, 359 (1998).
[55] G. M. Viswanathan, S. V. Buldyrev, E. K. Garger, V. A. Kashpur, L. S. Lucena, A. Shlyakhter, H. E. Stanley, and J. Tschiersch, Phys. Rev. E **62**, 4389 (2000).
[56] E. Koscielny-Bunde, A. Bunde, S. Havlin, H. E. Roman, Y. Goldreich, and H. J. Schellnhuber, Phys. Rev. Lett. **81**, 729 (1998).
[57] E. Koscielny-Bunde, H. E. Roman, A. Bunde, S. Havlin, and

H. J. Schellnhuber, Philos. Mag. B **77**, 1331 (1998).
[58] K. Ivanova, M. Ausloos, E. E. Clothiaux, and T. P. Ackerman, Europhys. Lett. **52**, 40 (2000).
[59] P. Talkner and R. O. Weber, Phys. Rev. E **62**, 150 (2000).
[60] Y. Ogata and K. Abe, Issues Sci. Technol. **59**, 139 (1991).
[61] M. F. Shlesinger and G. H. Weiss, *The Wonderful World of Stochastics: A Tribute to Elliott W. Montroll* (North-Holland, New York, 1985).
[62] D. Stauffer and H. E. Stanley, *From Newton to Mandelbrot*, 2nd ed. (Springer-Verlag, Berlin, 1996).
[63] H. A. Makse, S. Havlin, M. Schwartz, and H. E. Stanley, Phys. Rev. E **53**, 5445 (1996).
[64] J. W. Kantelhardt, E. Koscielny-Bunde, H. H. A. Rego, S. Havlin, and A. Bunde, Physica A **294**, 441 (2001).
[65] Z. Chen, P. Ch. Ivanov, K. Hu, and H. E. Stanley (unpublished).
[66] H. E. Hurst, Trans. Am. Soc. Civ. Eng. **116**, 770 (1951).
[67] B. B. Mandelbrot and James R. Wallis, Water Resources Res. **5**, No. 2, 321 (1969).
[68] P. Bernaola Galván, R. Román Roldán, and J. L. Oliver, Phys. Rev. E **53**, 5181 (1996).